Atmos. Chem. Phys. Discuss., 13, 1609–1672, 2013
www.atmos-chem-phys-discuss.net/13/1609/2013/
doi:10.5194/acpd-13-1609-2013

Atmospheric
Chemistry
and Physics
Discussions

Constraints on emissions of carbon monoxide, methane, and a suite of hydrocarbons in the Colorado Front Range using observations of $^{14}CO_2$

B. W. LaFranchi[1], **G. Pétron**[2,3], **J. B. Miller**[2,3], **S. J. Lehman**[4], **A. E. Andrews**[2], **E. J. Dlugokencky**[2], **B. R. Miller**[2,3], **S. A. Montzka**[2], **B. Hall**[2,3], **W. Neff**[3,5], **C. Sweeney**[2], **J. C. Turnbull**[6], **D. E. Wolfe**[5], **P. P. Tans**[2], **K. R. Gurney**[7], and **T. P. Guilderson**[1]

[1]Center for Accelerator Mass Spectrometry (CAMS), Lawrence Livermore National Laboratory, Livermore, CA 94550, USA
[2]Global Monitoring Division (GMD), NOAA Earth Systems Research Laboratory, Boulder, CO 80305, USA
[3]Cooperative Institute for Research in Environmental Sciences (CIRES), University of Colorado, Boulder, CO 80309, USA
[4]Institute for Arctic and Alpine Research (INSTAAR), University of Colorado, Boulder, CO 80305, USA
[5]Physical Sciences Division, NOAA Earth Systems Research Laboratory, Boulder, CO 80305, USA

[6]National Isotope Centre, GNS Science, Lower Hutt 5040, New Zealand
[7]School of Life Sciences, Arizona State University, Tempe, AZ 85287, USA

Received: 6 December 2012 – Accepted: 14 December 2012 – Published: 15 January 2013

Correspondence to: B. W. LaFranchi (lafranchi2@llnl.gov)

Published by Copernicus Publications on behalf of the European Geosciences Union.

Abstract

Atmospheric radiocarbon (^{14}C) represents an important observational constraint on emissions of fossil-fuel derived carbon into the atmosphere due to the absence of ^{14}C in fossil fuel reservoirs. The high sensitivity and precision that accelerator mass spectrometry (AMS) affords in atmospheric ^{14}C analysis has greatly increased the potential for using such measurements to evaluate bottom-up emissions inventories of fossil fuel CO_2 (CO_2ff), as well as those for other co-emitted species. Here we use observations of $^{14}CO_2$ and a series of hydrocarbons and combustion tracers from discrete air samples collected between June 2009 and September 2010 at the National Oceanic and Atmospheric Administration Boulder Atmospheric Observatory (BAO; Lat: 40.050° N, Lon: 105.004° W) to derive emission ratios of each species to CO_2ff. From these emission ratios, we estimate emissions of these species by using the Vulcan CO_2ff high resolution data product as a reference. The species considered in this analysis are carbon monoxide (CO), methane (CH_4), acetylene (C_2H_2), benzene (C_6H_6), and C_3–C_5 alkanes. Comparisons of top-down emissions estimates are made to existing inventories of these species for Denver and adjacent counties, as well as to previous efforts to estimate emissions from atmospheric observations over the same area. We find that CO is overestimated in the 2008 National Emissions Inventory (NEI, 2008) by a factor of ~ 2. A close evaluation of the inventory suggests that the r[illegible] of CO emitted per unit fuel burned from on-road gasoline vehicles is likely over-estimated by a factor of 2.5. The results also suggest that while the oil and gas sector is the largest contributor to the CH_4 signal in air arriving from the north and east, it is very likely that other sources, including agricultural sources, contribute to this signal and must be accounted for when attributing these signals to oil and gas industry activity from a top-down perspective. Our results are consistent with ~ 60 % of the total CH_4 emissions from regions to the north and east of the BAO tower stemming from the oil and gas industry, equating to ~ 70 Gg yr^{-1} or ~ 1.7 % of total natural gas production in the region.

Title Page
Abstract | Introduction
Conclusions | References
Tables | Figures
|◀ | ▶|
◀ | ▶
Back | Close
Full Screen / Esc
Printer-friendly Version
Interactive Discussion

1 Introduction

Radiocarbon in CO_2 ($^{14}CO_2$) is a powerful tracer that provides the least biased and most direct means to observe fossil fuel derived CO_2 in the atmosphere (Zondervan and Meijer, 1996; Hsueh et al., 2007; Levin and Karstens, 2007; Turnbull et al., 2009; Van der Laan et al., 2010). Fossil fuels are completely devoid of ^{14}C, as is the CO_2 resulting from its combustion, because the half life of ^{14}C is short (~ 5700 yr, Godwin, 1962) in relation to the residence times of carbon in fossil reservoirs, where no additional ^{14}C production occurs. Since all other sources of CO_2 to the atmosphere stem from carbon reservoirs that are in near equilibrium with the isotopic composition of the atmosphere itself, the atmosphere exhibits gradients in $^{14}CO_2$ that can be quantitatively traced to addition of CO_2 from fossil fuel combustion (Turnbull et al., 2007; Graven et al., 2009; Levin et al., 2010).

Prior to nuclear weapons testing, which artificially increased the $^{14}CO_2$ content of the atmosphere, the rise in atmospheric CO_2 resulting from fossil fuel combustion could be observed on global scales as a decrease in $^{14}CO_2$, widely known as the Seuss effect (Suess, 1955). While $^{14}CO_2$ is produced naturally in the upper atmosphere from cosmogenic radiation, the abundance of $^{14}CO_2$ in the modern atmosphere was strongly impacted by above ground nuclear testing that occurred in the middle part of the 20th century. Since the atmospheric nuclear weapons test ban was put in place, the decrease in $^{14}CO_2$, which has been observed at a number of global background monitoring sites (Levin and Kromer, 2004; Turnbull et al., 2007; Currie et al., 2011; Graven et al., 2012a,b), has been influenced primarily by the equilibration of atmospheric $^{14}CO_2$ with the oceanic and terrestrial carbon reservoirs. In recent years, however, the atmospheric decline has been dominated increasingly by isotopic dilution due to the Seuss effect, as fossil fuel combustion increases and as the atmosphere, ocean, and terrestrial carbon reservoirs approach equilibrium with the “bomb spike”. On regional scales, locally emitted CO_2 from fossil fuel combustion can be detected as a depletion of $^{14}C:^{12}C$ relative to background air. These observed gradients result from what we define as "recently added" fossil-fuel CO_2 (CO_2ff).

Observations of $^{14}CO_2$ are of great interest, not only for the evaluation of fossil CO_2 emissions inventories, but also as a means to better understand emissions of a range of trace gases associated with the combustion of fossil fuels (Turnbull et al., 2011; Miller et al., 2012). Bottom-up inventories of these trace gases carry significant uncertainties because of the difficulty in quantifying the relationship between the mass of fuel consumed and the mass of trace gas emitted. Emissions of by-products, including species such as carbon monoxide (CO), methane (CH_4), acetylene (C_2H_2), and benzene (C_6H_6) depend on a number of variables including fuel type, combustion temperature, the extent of tail-pipe or flue-stack "scrubbing", and oxidant-to-fuel ratio. For example, it has long been known from observations that the National Emissions Inventory (NEI) appears to over-estimate observed anthropogenic emissions of CO in the United States (Parrish, 2006; Hudman et al., 2008; Miller et al., 2008, 2012), though the reason remains unclear. Further, there are a number of industrial activities that lead to non-combustion emissions of gases impacting air quality and climate from leaks in transmission lines, venting of storage tanks, and other processes, in which case, quantifying emissions based on readily available fuel use statistics is difficult or not possible. In contrast, the amount of CO_2 emitted per unit of fuel combusted can be derived stoichiometrically with relatively high accuracy. Accordingly, the bottom-up inventory of fossil fuel derived CO_2 in the United States (e.g. EIA, 2012) and in most developed countries is thought to be relatively reliable. Estimates of annual fossil CO_2 emissions for the US are thought to be reliable to $\sim 10\,\%$ (1σ) (Gurney et al., 2011), though uncertainties are larger at smaller spatial and temporal scales.

To improve emissions estimates for these other combustion and industrial tracers, particularly those species that can affect air quality, human health, and climate, observations in the atmosphere are necessary for critically evaluating the existing bottom-up inventories. One relatively simple strategy for deriving emissions based on atmospheric observations is the use of tracer/tracer enhancement ratios in which emission ratios of two species are inferred from the ratio of the observed mole fraction enhancements (with respect to background observations) of one species to the other. For gases with lifetimes comparable to the transit times between emission and measurement, a simple photochemical age model can be used to extrapolate back from the time of the observation to derive the ratio at the time of emission (Lee et al., 2006; Warneke et al., 2007). Then, if emissions of one of the tracers are relatively well defined for the geographic area that the observations are sensitive to, emissions of the other tracer can be calculated from the inferred emission ratio. Uncertainties for this method are minimized when both tracers have long atmospheric lifetimes and slow atmospheric production rates on the time scales relevant to the source-receptor distances. A major advantage of this approach comes from its computational simplicity. Additionally, since all tracers are expected to be mixed and transported in the same way if their sources are co-located, this approach reduces the sensitivity of the analysis on uncertainties in transport and boundary layer calculations.

The very long atmospheric chemical lifetime of CO_2 would be ideal for use in these tracer/tracer approaches, but large uncertainties in its biogenic sources and sinks can complicate its use in inferring emissions of other fossil fuel combustion tracers (e.g. Miller et al., 2012). Thus, to take advantage of the photochemical stability of CO_2 and the availability of relatively accurate fossil fuel CO_2 emissions inventories measurements of $^{14}CO_2$ must be used to isolate the fossil fuel contribution to the observed CO_2. Here we describe observations of $^{14}CO_2$ and other trace gases made between late June 2009 and September 2010 at the Boulder Atmospheric Observatory (BAO), a 300 m tall tower located 35 km north of Denver, CO (Lat 40.05N, Lon 105.01W). BAO is one of 9 towers in the NOAA Earth System Research Laboratory Global Monitoring Division (NOAA-GMD, hereafter) tall tower network (Andrews et al., 2013). It is one of 7 towers in the network that is monitoring CO_2 and CO continuously and collecting air samples daily for multiple species analysis and one of 6 that also measures $^{14}CO_2$. The observations presented here represent the first report of $^{14}CO_2$ observations from this network. In this study, we use $^{14}CO_2$ to derive CO_2ff mole fractions for estimating

Title Page
Abstract Introduction
Conclusions References
Tables Figures
◀ ▶
◀ ▶
Back Close
Full Screen / Esc
Printer-friendly Version
Interactive Discussion

emission ratios and emissions of a number of important trace gases being transported to the site from the Denver metro region and from the extensive oil and gas drilling operations and cattle feedlots in Weld County, to the northeast.

This study builds on a previous effort to characterize emissions of volatile organic compounds (VOCs) and CH_4 from oil and gas production and drilling operations in Weld County using both bottom-up and top-down approaches for 2008 (Pétron et al., 2012). We will refer to this prior study as the Colorado Front Range Pilot Study (CFRPS, hereafter), in which the authors made use of observations at BAO in combination with those from a mobile platform to determine emission signatures of individual methane sources, including oil and gas wells, natural gas processing plants, condensate storage tanks, landfills, cattle feed-lots, and waste water treatment plants. A crucial finding of the CFRPS is that trace gas concentrations measured at BAO are influenced most substantially by two different source regions: oil and gas fields in Weld County (from a region known as the Denver Julesberg Basin, or DJB) and urban-type emissions from the Denver metro region. They found that air arriving at BAO from the northeast exhibits strong enhancements in alkanes, including methane, resembling enhancements (based on tracer/tracer ratios) similar to those sampled on the mobile platform within the DJB. These results suggested that oil and gas operations are the dominant emitters of alkanes and methane in the region and that the observations at BAO provide reliable constraints on emissions from these activities.

The CFRPS estimated emissions from the DJB using a tracer/tracer approach with constraints set by bottom-up statistical data on methane and propane emissions from a subset of condensate tanks in the region and a survey of raw natural gas composition. The confidence in these estimates is ultimately limited by uncertainties in the average composition of gas released from a representative sub-set of condensate tanks and oil and gas wells exhibiting a wide range of compositions. In a separate evaluation of the data analyzed in the CFRPS, Levi (2012) (denoted as L12, hereafter) using a slightly different approach making use of *n*-butane data in addition to methane and propane, estimated CH_4 emissions that are substantially lower than the CFRPS estimates and are more in line with the bottom-up estimates. Here, we add to the characterization of trace gas emissions in the DJB, as well as in the Denver metro region, by using radiocarbon-derived CO_2ff observations as an improved constraint that is independent of the assumptions made in these two prior studies. The primary advantage of the approach taken here is that by using the Vulcan fossil fuel CO_2 data product (Gurney et al., 2009) as a quantitative reference, which is reliable nationwide to within 20 % at the county level on annual time-scales, our confidence in the reference emissions estimate is greatly improved. Further, as we will show, CO_2ff exhibits strong correlations with a variety of trace gases in the region, both from combustion and non-combustion sources, thus allowing for the evaluation of emissions from a range of different source-types.

2 Methods

2.1 Site description

The BAO tower is located 25 km east-northeast of Boulder and 35 km north of Denver (40.05° N, 105.01° W). The base of the tower is at 1584 m a.s.l. (above sea level). As shown in Fig. 1, BAO is located at the southwestern edge of the DJB where a very large and dense network of oil and gas wells exists. Since late 2007 NOAA-GMD has been collecting discrete air samples approximately daily from 300 m. The air is collected in glass flasks and analyzed at NOAA-GMD for a suite of ~ 50 trace gases and then circulated to the University of Colorado's Institute of Arctic and Alpine Research (INSTAAR) for stable isotope measurements in CO_2 and CH_4 and preparation for $^{14}CO_2$ measurement. The Center for Accelerator Mass Spectrometry (CAMS) at Lawrence Livermore National Laboratory (LLNL), which performed the $^{14}CO_2$ measurements reported here, has participated in the NOAA-GMD $^{14}CO_2$ discrete air sample measurement program since 2009. This study focuses on data collected between late June 2009 and September 2010, over which time 145 samples were analyzed for $^{14}CO_2$. More information on this site and the entire tall tower network (Andrews et al., 2013) can be found at: http://www.esrl.noaa.gov/gmd/ccgg/towers/.

Standard meteorological measurements are also made continuously at several levels on the tower by the NOAA ESRL Physical Sciences Division, including wind speed and direction, relative humidity, and temperature. We categorize each observation in our analysis according to wind direction in order to facilitate a discussion of two distinct emission source regions: the oil and gas industrial region to the north and east and the Denver metro region to the south. To do this, we define three wind sectors, consistent with those defined in the CFRPS: N/E (345° to 120°), S (120° to 240°), and W (240° to 345°). These wind sectors are illustrated in Fig. 1. Wind direction for each sample is determined using the mean wind direction over the 30 min immediately prior to sampling. Samples with mean wind speeds lower than 2.5 $\mathrm{m\,s^{-1}}$ over this time period are removed from any sector-specific analysis in this study.

To define isotopic and mole fractions of trace gases in background air, measurements from two additional sites were used. For $^{14}CO_2$, CO_2, CO, and CH_4, we used weekly measurements from Niwot Ridge, CO (sitecode NWR, 40.05° N, 105.63° W, 3526 m a.s.l.), a site in the alpine tundra with strong westerly winds that only rarely required filtering of samples influenced by pollution from the Denver metro area (Turnbull et al., 2007). For other gases, including acetylene, benzene, and the C_3–C_5 alkanes we used weekly to fortnightly samples collected in the free troposphere from flights at a nearby location (3000 to 4000 m a.s.l. above Briggsdale Colorado; sitecode CAR, 40.37° N, 104.30° W, ground elevation ~ 1700 m a.s.l.).

2.2 Flask sampling

Discrete whole air samples are collected daily (Andrews et al., 2013) from the BAO tall tower (at the 300 m level) using Programmable Flask Packages (PFPs) connected to a Programmable Compressor Package (PCP) capable of delivering 15 standard $\mathrm{L\,min^{-1}}$. Each PFP contains 12 cylindrical borosilicate glass flasks (0.7 L each). On each end of the flasks are automated glass-piston stopcocks, sealed with Teflon Orings. Prior to deployment, each flask in the PFP unit is flushed with clean dry air and then pressurized to ~ 140 kPa with synthetic air containing 330 ppm CO_2.

Automated sampling consists of the following steps: (1) a manifold flush, (2) a flask flush, and (3) pressurization of the flask to ~ 270 kPa. The entire process takes about 2 min. Sampled air at BAO first passes through a drying stage (dewpoint temperature at ambient pressure of ~ 5 °C) prior to collection. Sampling is done at midday (19:30 UTC) in most cases; all samples used in this analysis were collected within about 30 min of 19:30 UTC. Two flasks are filled within 5 min of each other (~ 4 standard liters) for analysis of the standard suite of trace gases (described below), with enough gas remaining for analysis of $^{14}CO_2$, which typically requires 0.4 to 0.5 mgC for high precision analysis.

2.3 Flask analysis

Each flask pair is analyzed at NOAA–GMD for CO_2, CO, CH_4, SF_6, H_2, N_2O, and a suite of halocarbons and hydrocarbons. Stable isotopes of CO_2 ($\delta^{13}C$ and $\delta^{18}O$) are analyzed at the INSTAAR Stable Isotope Laboratory (Vaughn et al., 2004). In this study, we use measurements of CO_2, CO, CH_4, acetylene (C_2H_2), benzene (C_6H_6), propane (C_3H_8), *n*-butane (n-C_4H_{10}), *n*-pentane (n-C_5H_{12}), and *i*-pentane (i-C_5H_{12}). We also use $\delta^{13}C$ in CO_2 in the calculation of $\Delta^{14}C$, according to methods described by Stuiver and Polach (1977).

Dry air mole fractions of CO_2, CH_4, and CO were measured on one of two nearly-identical custom automated analytical systems. These systems consist of custom-made gas inlet systems, gas-specific analyzers, and system-control software. During this project, each system used a different technique to measure CO. One used a Reduction Gas Analyzer, where CO is separated from air by gas chromatography, then passed through a heated bed of HgO producing Hg before it is detected by resonance absorption (Novelli et al., 1998). The second is Vacuum UV Resonance Fluorescence (VURF), where CO is detected by fluorescence at ~ 150 nm. Both techniques are calibrated against the same standard scale, and uncertainties (68 % confidence interval) are ~ 1 ppb for the VURF and ~ 2 ppb for the RGA. Long-term comparison of the two systems show the RGA and VURF agree within ~ 1 ppb. CH_4 was measured by gas chromatography (GC) with flame ionization detection with an uncertainty of ~ 1.4 ppb (Dlugokencky et al., 1994). A non-dispersive infrared analyzer is used for CO_2 with an uncertainty < 0.1 ppm (Conway et al., 1994).

The hydrocarbons (C_2H_2, benzene, and C_3–C_5 alkanes) are measured using a GC/mass spectrometric technique, with cryogenic pre-concentration (Montzka et al., 1993). Relative measurement uncertainties for the hydrocarbons considered in this study vary depending on mole fraction, with lower relative uncertainties estimated for samples with lower mole fractions (down to 10 ppt). For mole fractions between 10 ppt and 1 ppb, uncertainties (1σ) are 5 % for i-C_5H_{12}, n-C_5H_{12}, and C_6H_6, and 15 % for C_3H_8, C_2H_2 and n-C_4H_{10}. At higher atmospheric mole fractions the uncertainties are larger: by a factor of two for mole fractions between 1 ppb and 20 ppb, and a factor of three for mole fractions between 20 ppb and 50 ppb. Only C_3H_8 was observed at mole fractions greater than 50 ppb during the study period; these 2 samples were removed from this analysis. The average relative uncertainties for individual samples are 5–8 % for i-C_5H_{12}, n-C_5H_{12}, and C_6H_6 and 15–30 % for C_3H_8, C_2H_2 and n-C_4H_{10} during the study period. Measurement repeatability (1σ) is generally < 2 % for compounds present at mole fractions > 10 ppt. For C_2H_2 and C_3H_8, the most volatile of these compounds, repeatability was somewhat poorer during these flask analyses (approx. −25 % and +12 %).

All measurements are reported as dry air mole fractions relative to internally consistent standard scales maintained at NOAA-GMD. We use the following abbreviations for measured dry air mole fractions: ppm = µmol (tracegas) mol (dryair)$^{-1}$, ppb = nmol mol^{-1}, and ppt = pmol mol^{-1}. Additional details on these methods are described at http://www.esrl.noaa.gov/gmd/ccgg/aircraft/analysis.html.

Title Page
Abstract Introduction
Conclusions References
Tables Figures
◀| |▶
◀ ▶
Back Close
Full Screen / Esc
Printer-friendly Version
Interactive Discussion

2.4 Radiocarbon analysis

A subset (typically 1 out of every 2 pairs) of the flask pairs are hand selected for analysis of $^{14}CO_2$. The selection is based on an analysis of continuous CO and CO_2 observations with the intent of selecting a combination of both locally-impacted and background samples. High precision measurements of $^{14}CO_2$ were made by extracting CO_2 from the whole air samples using cryogenic separation, reducing the extracted CO_2 to graphite for atom counting via accelerator mass spectrometry (AMS). Extractions of authentic samples, measurement controls, and process blanks were performed at the University of Colorado INSTAAR Laboratory for AMS Radiocarbon Preparation and Research (NSRL) using an automated extraction system (Turnbull et al., 2010). Graphitization and AMS analysis was done at LLNL-CAMS. A description of the high precision methods for analysis of atmospheric samples at CAMS is given by Graven et al. (2007). The measurements are expressed as age-corrected $\Delta^{14}CO_2$ in units of per mil (‰), calculated from the $^{14}C/^{13}C$ ratio, measured relative to NBS Oxalic Acid I (OX1) and reported relative to the absolute radiocarbon standard (1890 wood), as detailed in Stuiver and Polach (1977).

Uncertainty in these observations is assigned as the standard deviation (1σ) of a series of repeat measurements on extraction aliquots of whole air stored in high pressure cylinders. Air from two surveillance cylinders having different but near-ambient ^{14}C activities, identified as NWT3 and NWT4, was extracted, graphitized, and analyzed concurrent with the BAO samples across 7 different measurement "wheels" or batches. Multiple samples of NBS Oxalic Acid II (OX2, a commonly used secondary standard) were combusted, graphitized and analyzed simultaneously. Typically, in a wheel containing 25 authentic samples, 12 measurement controls and 1 process blank were analyzed. For the observations described in this study, the (1σ) repeatability (standard deviation) of NWT3 and NWT4 samples was ±2.2‰. In a small number of cases, the internal variability of repeat measurements of the same sample was larger than the repeatability of the pool of NWT samples. The larger of the two is assigned as the uncertainty for a given $\Delta^{14}CO_2$ measurement.

2.5 Calculation of CO_2ff

Recently added fossil fuel CO_2 (CO_2ff) is defined as the local enhancement of CO_2, with respect to an appropriate background reference site, due to fossil fuel emissions. CO_2ff is estimated using a mass balance approach (Levin et al., 2003), in which the observed mole fraction of CO_2 (CO_2obs) is partitioned into background CO_2 (CO_2bkg), fossil CO_2, and biogenic CO_2 (CO_2bio) components. CO_2bio is the net balance between respired CO_2 (CO_2resp) and CO_2 taken up by photosynthesis (CO_2photo). We further separate the respired fraction into autotrophic respiration (CO_2auto) and heterotrophic respiration (CO_2het) that originates from older soil carbon pools (which typically contain more bomb ^{14}C). Equations (1a) and (1b) detail this mass balance relationship, as formulated in Turnbull et al. (2006) and also described in Miller et al. (2012), with CO_2resp separated into heterotrophic and autotrophic components. Similarly, an isotopic mass balance equation (Eq. 2) can describe the contribution of these three end members to the total observed $\Delta^{14}C$.

$$CO_2\text{obs} = CO_2\text{bkg} + CO_2\text{ff} + CO_2\text{bio} \tag{1a}$$

$$CO_2\text{bio} = CO_2\text{auto} + CO_2\text{het} - CO_2\text{photo} \tag{1b}$$

$$\Delta^{14}_{\text{obs}}CO_2\text{obs} = \Delta^{14}_{\text{bkg}}CO_2\text{bkg} + \Delta^{14}_{\text{ff}}CO_2\text{ff} + \Delta^{14}_{\text{bio}}CO_2\text{bio} \tag{2}$$

Since $\Delta^{14}C$ values are all normalized by their $\delta^{13}C$ values, and thus are not influenced by natural fractionation, we can assume that $\Delta^{14}_{\text{photo}}$ and $\Delta^{14}_{\text{auto}}$ are identical to Δ^{14}_{bkg} (Turnbull et al., 2006). The system of equations can then be solved for CO_2ff to give Eq. (3).

$$CO_2\text{ff} = \left(\frac{CO_2\text{obs}(\Delta^{14}_{\text{obs}} - \Delta^{14}_{\text{bkg}})}{(\Delta^{14}_{\text{ff}} - \Delta^{14}_{\text{bkg}})}\right) - \left(\frac{CO_2\text{het}(\Delta^{14}_{\text{het}} - \Delta^{14}_{\text{bkg}})}{(\Delta^{14}_{\text{ff}} - \Delta^{14}_{\text{bkg}})}\right) \tag{3}$$

In this equation, the variables in the first term are either known ($\Delta^{14}_{\mathrm{ff}} = -1000$ ‰) or can be measured. We use observations from NWR to estimate $\Delta^{14}_{\mathrm{bkg}}$. The background estimate is calculated by applying a smoothing algorithm (Thoning et al., 1989) to the NWR data (a curve-fit of 3 polynomials, 4 harmonics, and added low-pass filtered residuals), after filtering out samples influenced by upslope flows carrying locally influenced air, characterized by high CO/$\mathrm{CO_2}$ ratios, as in Turnbull et al. (2007). The selection of a proper background site introduces uncertainties on the order of the measurement uncertainty ($\sim$ 2 ‰) (Turnbull et al., 2009). The second term in Eq. (3) is a minor correction to the calculation of $\mathrm{CO_2}$ff due to heterotrophic respiration from soils, which can draw from carbon pools that are on the order of 10 yr old and, thus, reflect the higher $\Delta^{14}\mathrm{CO_2}$ in the atmosphere at the time. The magnitude of this correction can be estimated from a terrestrial ecosystem model, such as the CASA biogeochemical model (Thompson and Randerson, 1999); we follow the estimates of Turnbull et al. (2009) for North American mid-latitudes and set this correction to −0.2 (±0.1) ppm (thus resulting in a positive offset) from October to March and to −0.5 (±0.3) ppm from April to September. Since the correction term in Eq. (3) is subtracted from the first term, the impact of heterotrophic respiration is to raise estimates of $\mathrm{CO_2}$ff in both seasons.

The influence of additional sources on Δ^{14}obs is globally variable and has potential contributions from stratospheric intrusion of cosmogenically produced and bomb-era ^{14}C (e.g. Levin et al., 2010; Graven et al., 2012a), nuclear reactors (e.g. Graven and Gruber, 2011), biomass burning (e.g. Schuur et al., 2003; Vay et al., 2011), and the oceanic-atmosphere disequilibrium (e.g. Sweeney et al., 2007; Muller et al., 2008). However, model-based estimates of the Δ^{14}C signal (not including those from nuclear emissions) in the conterminous United States (Miller et al., 2012) show that these terms contribute very little relative to the spatial gradients arising from fossil fuel combustion. Graven and Gruber (2011) argue that in the eastern United States nuclear contributions may be significant, but they predict near-zero nuclear influence in most of the western United States, including Colorado. Any contribution from stratosphere or ocean sources at BAO is likely to simultaneously impact the NWR background site and, thus, can be ignored in this analysis. At least one sample was influenced by a biomass burning event, identified by an anomalously high CO/CO_2ff ratio, as well as multiple news reports of poor air quality on that particular day resulting from the Station Fire in southern California in August 2009 (e.g. Brennan, 2009). This sample, along with one other that exhibits an abnormally high CO/CO_2ff ratio is omitted from this analysis. The sample influenced by the wildfire plume was collected 1 September 2009; the other sample, collected 30 January 2010, is unusual in that the estimated CO_2bio mole fraction was very large (15 ppm), and about twice the estimated CO_2ff for this sample. The large CO_2bio relative to other samples in the data set suggests the possibility of an undetected stratospheric or biomass burning influence or an unusually large heterotrophic respiration signal, therefore we exclude this point from our analysis. In addition to CO, a large number of other anthropogenic tracers were elevated in this particular sample.

2.6 Bottom-up fossil fuel CO_2 emissions estimates

To derive top-down emissions estimates for the observed trace gases via tracer/CO_2ff enhancement ratios, we use both county-level and gridded bottom-up fossil fuel CO_2 emissions estimates from the Vulcan data product (v2.2) (Gurney et al., 2009) as a quantitative reference. Vulcan (http://vulcan.project.asu.edu) is a high resolution data product that utilizes a combination of energy, air quality, census, traffic, and digital road statistics to quantify fossil fuel CO_2 emissions for the United States. Until recently, the Vulcan inventory was available only for 2002, but is now updated to include annual emissions at the county and state level for all years between 1999 and 2008. The gridded high resolution product is currently available only for 2002, however. Since we make use of both the county-level and gridded inventories in our analysis, the Vulcan02 data product is used as the base year for consistency. For the Vulcan02 product, country-wide, emissions are in agreement with the United States Energy Information Administration (EIA) estimates to about 2 % even though these emissions were compiled using two different independent statistical data sets (Gurney et al., 2011). At the county level, the estimated uncertainty (1σ) on annual CO_2ff emissions from the Vulcan02 data product is variable, but no more than ~ 20 % (and typically less than ~ 10 %) for any given county (Gurney et al., 2011). To apply the Vulcan02 data product to our analysis period (2009–2010), the Vulcan02 emissions are scaled up to the observation period using the state-level EIA inventory (EIA, 2012), which is currently available through 2009. We use the county-level Vulcan data product for 2003–2008 to constrain the uncertainty in our scaling factor derived from the state-level EIA data. A more detailed description of the scaling procedure and associated uncertainty is provided below (Sect. 3.3).

Vulcan emission rates for CO_2 are given in Table 1 for two source regions that correspond to the N/E and S wind sectors, as defined above (Sect. 2.6). For simplicity we define the N/E wind sector as being influenced primarily by emissions from Weld and Larimer Counties and the S wind sector as being influenced primarily by emissions from Adams, Broomfield, Arapahoe, Jefferson, and Denver Counties (collectively referred to here as the Denver metro counties). Total CO_2ff emissions, according to Vulcan02, are estimated to be 2.94 Tg C and 7.27 Tg C for the [illegible]E (Weld and Larimer Counties) and S (Denver metro counties) wind sectors, respectively.

2.7 Bottom-up trace gas emissions estimates

We compare our top-down emission estimates with bottom-up data, where available, for each tracer species, including: CO (NEI, 2008), acetylene (NEI, 2005), benzene (NEI, 2008 and CFRPS), CH_4 (EDGAR v4.2 2008 and CFRPS), and the C_3–C_5 alkanes (NEI, 2005 and CFRPS). Emissions of C_2H_2 and the C_3–C_5 alkanes are estimated from a gridded NEI 2005 inventory of total VOC emissions in combination with the EPA SPECIATE(v4.3) model (EPA, 2011). Additional estimates of certain gases are provided in the CFRPS, which derived a bottom-up inventory for benzene, CH_4, and the C_3–C_5 alkanes representing emissions from flashing of condensate storage tanks and venting of natural gas wells in Weld County in 2008. These emissions estimates were derived from total VOC emissions estimates from the WRAP/Environ inventory (Bar-Ilan et al., 2008a, b) in combination with a series of speciation profiles of raw natural gas (for venting emissions) and condensate tank mixtures (for flashing emissions) in the region. From the various speciation profiles available, average emissions were calculated for each along with the maximum and minimum values, thus giving a range of bottom-up estimates (Pétron et al., 2012). As we will discuss below, the CFRPS bottom-up inventory is a compilation of emissions from oil and gas related activities only, but other important sources exist for some species, in particular for benzene and methane.

Table 1 summarizes the bottom-up emission estimates, including the base-year for each inventory. Scaling factors (α) for the trace gases that relate the inventory base-year to the observation period are estimated from population statistics or additional factors. Scaling of the tracer inventories related primarily to mobile emissions (i.e. CO, benzene, and C_2H_2) is calculated in proportion to the rate of increase in population according to statistics from the US Census Bureau. For these species, uncertainty limits for the scaled emissions are assigned as the base year estimates (i.e. no change in emissions) on the low end to an estimate using a scaling factor that is 3 times the population increase on the high end. The one exception to this is for the uncertainty limits for CO emissions. There is evidence that on road mobile CO emissions have decreased in many urban regions over the past 15–20 yr despite large population increases, and in Denver, specifically, the CO-to-fuel burnt ratio was observed to have decreased at a rate of about 7 % per year between 1999 and 2007 (Bishop and Stedman, 2008). Therefore, the bottom-up CO emissions uncertainty is bracketed at the low end by an emission rate corresponding to a decrease in emissions of 10.5 % from 2008 (the inventory base year) to the observation period. For CH_4 and the C_3–C_5 alkanes, emissions in Weld/Larimer counties are scaled by increases in gas and oil production (by total dollar amount), according to statistics from the Colorado Oil and Gas Conservation Commission (COGCC, 2011). Uncertainties for the CFRPS base-year estimates represent the minimum (un-scaled) and maximum (scaled) values, given a set of 3 speciation profiles based on measured raw natural gas composition data for 77 wells (COGCC, 2007) and a set of 16 modeled flash emissions profiles for condensate tanks (provided by CDPHE, see details in Pétron et al., 2012). These uncertainties are modified here to reflect the additional uncertainty resulting from up-scaling to the observation period. Since virtually all the gas and oil wells in the Weld/Larimer county region are located in Weld county (99.8 % of the total production, according to the COGCC), the CFRPS estimates, which correspond to Weld county emissions alone, are taken to represent the total Weld/Larimer emission rate. For the South wind sector, where the oil and gas industry is likely the source of only a small percentage of emissions, the EDGARv4.2 (EDGAR hereafter) 2008 CH_4 and NEI 2005 C_3–C_5 inventory emission estimates are scaled in accordance with population increases, with uncertainties assigned as described above for trace gases related to mobile emissions. We acknowledge that scaling up of these trace gas estimates is an unconstrained approximation, especially for species such as benzene and methane, which have multiple unrelated sources that likely do not scale linearly. For this reason we have taken a conservative approach in assigning scaling uncertainties. It is important to note, however, that the inventory base year estimate is always within the uncertainty brackets of the scaled inventory values, thus allowing the reader to evaluate the top-down and bottom-up comparison independent of any scaling assumptions made here.

3 Results and discussion

3.1 Δ^{14}C and CO_2ff time series

The results of the $^{14}CO_2$ analyses are shown in Fig. 2a with values ranging from −19.4 to 50.5‰. The time series runs from late June 2009 to September 2010, overlapping with the observation period of the CFRPS, where observations (from the same set of flask samples) up through the spring of 2010 were included their top-down emission calculations. Excursions of $\Delta^{14}CO_2$ at BAO (relative to the NWR background site) towards lower values signify the addition of recently emitted fossil fuel CO_2 to the sampled air mass. As described in Sect. 2.5, the CO_2ff mole fraction can be quantified using Eq. (3), with an uncertainty of 1.2 ppm based on propagation of the analytical uncertainty in $\Delta^{14}CO_2$ for both Δ^{14}obs and Δ^{14}bkg (the uncertainty in CO_2 terms is small relative to those for $\Delta^{14}C$). Performing this calculation for each BAO observation in Fig. 2a gives CO_2ff mole fractions that range from below the 1.2 ppm detection limit up to 25 ppm. There are instances of negative CO_2ff values (14 % of all samples), which is not physically realistic, in the dataset. All but 5 of these samples (3 % of the entire data set) lie within the 1σ envelope around zero and only 1 sample (–3.3 ppm) lies outside of 2σ.

The most obvious feature of the CO_2ff variability is that mole fractions are high and variable in the winter months and relatively constant and lower, on average, during the summer months (Fig. 2b). This trend is qualitatively consistent with shallow, and variable, boundary layer heights in the winter and deep boundary layers in the summer. Boundary layer height is driven by a number of complex meteorological and topographical variables, but largely by surface sensible heat flux, which is of course much lower during the winter. Tracer/tracer ratios are expected to be much less sensitive to variability in boundary layer height since the dilution and mixing of co-located emissions will impact the different tracers equally. As we describe below, observations of a set of tracer/CO_2ff ratios are consistent with this expectation.

3.2 Variability in tracer/CO_2ff enhancement ratios

When sources of trace gas emissions are co-located with fossil fuel combustion sources, an analysis of the trace gas abundances relative to CO_2ff provides a means to better understand the variability in the mix of emission sources influencing the site independent of the dilution and mixing dynamics that impact absolute mole fractions. An alternate explanation could be that emissions of all the trace gases have similar seasonal cycles to CO_2ff. Tracer/CO_2ff enhancement ratios are calculated here by taking the median of individual tracer/CO_2ff ratios after subtracting the background from each trace gas. The median emission ratio derived from all samples provides a more robust estimate of the apparent tracer/CO_2ff ratios than that determined from either a linear regression slope or an arithmetic mean, which give estimates that are overly sensitive to ratio outliers that can result from signals due to air masses in which emissions of various sources are not well mixed (Miller et al., 2012). Samples are only used in the ratio calculation when estimated CO_2ff is above the 1.2 ppm 1σ detection limit. Uncertainties in the median ratios are 95 % confidence intervals, defined as the 2.5–97.5 percentile range (~ 2σ confidence) from a distribution of 500 estimates of the median from a randomized re-sampling of the data (boot-strapping with replacement). We also estimated the uncertainty in the tracer/CO_2ff enhancement ratios associated with measurement uncertainty (both for the trace gas and CO_2ff) and found that these uncertainties (at 2σ) were comparable or lower than the boot-strap approach in all cases. A measure of the appropriateness of this approach is estimated by calculating the coefficient of determination (r^2) from a linear regression of tracers vs. CO_2ff; a high r^2 suggests that emissions of the tracers are appreciably co-located with fossil fuel combustion sources. Results from the tracer/CO_2ff enhancement ratio calculations (with associated uncertainties and r^2 values) are detailed in Table 1. Background observations for the different trace gases are taken from one of two nearby sites in the NOAA-GMD global network, either NWR (CO and CH_4) or from flights at CAR (acetylene, benzene, and the C_3–C_5 alkanes). CO and CH_4 observations are available from both sites and we confirmed that the enhancement ratio estimates are not appreciably sensitive to the selection of background site (differences between 7 % and 15 % in derived enhancement ratios).

The sensitivity of this analysis to the prescribed heterotrophic respiration correction to CO_2ff (Eq. 3) was determined by recalculating the tracer/CO_2ff ratios with this correction term doubled, in one case, and set to zero in another. The ratios estimated from this sensitivity test were within the 95 % confidence intervals in all but one case. The lone exception was the CH_4/CO_2ff ratio for the N/E wind sector, where the recalculated ratio using a respiration correction of zero is 34.1 ppb/ppm compared to the base case upper confidence limit of 33.4 ppb/ppm, extending the upper uncertainty limit by only 2 %. Thus we consider the uncertainty in the heterotrophic respiration correction to CO_2ff a largely insignificant source of error in our analysis. Given the relative lack of vegetation in the region surrounding BAO, it is more likely that the prescribed respiration correction is biased high rather than low, which would result in CO_2ff values that are biased high and tracer/CO_2ff enhancement ratios that are biased low.

While variability in the absolute mole fractions of the tracers and CO_2ff has a strong seasonal dependence (e.g. Fig. 2b), with larger enhancements observed in the winter than the summer, there is no apparent seasonality to any of the considered tracer/CO_2ff enhancement ratios, suggesting that boundary layer dynamics are largely what are driving the seasonality in measured atmospheric mole fractions. As we discuss below, the primary source of variability in the tracer/CO_2ff enhancement ratios at BAO is due to changes in wind direction, with significantly different tracer signatures observed when air is transported from Weld and Larimer counties to the north and east (N/E) vs. from the Denver metro region to the south (S). A relatively small number of samples in this data set arrived from the W wind sector, most of which did not have very strong enhancements of CO_2ff or other trace gases. We therefore ignore these samples in our analysis.

Previous work (Pétron et al., 2012) found significant differences in mole fractions of alkanes, including CH_4, C_3H_8, n-C_4H_{10}, i-C_5H_{12}, and n-C_5H_{12}, observed at BAO as a function of wind direction and related differences in emission sources. Benzene was also found to be enhanced in air masses arriving from the N/E. These differences were attributed to oil and gas production in Weld County, to the northeast of BAO. As shown on the map in Fig. 1, the majority of these wells are located in Weld County (SkyTruth, 2008), from which 17.9 million barrels of oil and 5.7 billion cubic meters of natural gas were produced in 2009 (COGCC, 2011). Other potential sources of CH_4 include cattle feedlots, landfills, waste water treatment plants, and natural gas processing plants. The transportation or mobile sector contributes significantly to a subset of the gases considered: CO, C_2H_2, C_6H_6, and i-C_5H_{12} (Watson et al., 2001). This sector likely contributes significantly to emissions from the Denver metro counties, but there are also significant mobile emissions in the N/E wind sector from Interstate 25, the main north-south route in Colorado, as well as in a number of population centers, including Fort Collins, all located due north of BAO, in Larimer County. Table 2 summarizes the expected sources of the trace gases evaluated in this analysis, along with their expected atmospheric lifetime with respect to oxidation by OH. Lifetimes of the tracers considered range from 3 days (pentanes) to 7 yr (CH_4) (at a modest OH molecular density of 10^6 cm^{-3}). The oxidation of tracers can potentially reduce the observed enhancement ratio resulting in a lowering of the presumed emission ratio; however, as we will discuss, we find no evidence of sufficient OH chemistry to impact the tracer/CO_2ff ratios discussed here.

3.2.1 Carbon monoxide

Figure 3a shows the relationship between CO and CO_2ff for each sample. Fits of a linear regression are included in the Fig. 3a for the N/E and S wind sectors, giving r^2 values of 0.75 ($n = 44$) and 0.85 ($n = 25$), respectively. As detailed in Table 1, and shown in Fig. 4, the point-by-point analysis of these observations show median (with 2σ confidence intervals) CO/CO_2ff enhancement ratios of 9.3 (8.1–10.6) and 10.0 (6.7–13.3) for the N/E and S wind directions, respectively. For all wind sectors combined, the median ratio is 9.3 (8.3–10.8) ($r^2 = 0.81$).

The observed ratios from both wind sectors are similar to the values of 6.8 ± 2.2 and 11.7 ± 5.5 ppb ppm^{-1} calculated at Niwot Ridge from two samples originating from the Denver area via upslope winds in 2004 (Turnbull et al., 2006). Our estimates are somewhat lower, however, than previous reported values of CO/CO_2ff in Denver, where ratios were derived from linear correlations across 4 different aircraft flights (~ 4–6 samples per flight) in May and July of 2004 (Graven et al., 2009). The observed ratios from these flights ranged from 14–27 ppb ppm^{-1}. While the well documented (e.g. Bishop and Stedman, 2008) reductions in CO emissions from mobile sources between 2004 and 2009 (part of a much longer term trend across most of the country) could be a factor in the lower enhancement ratios observed here, the long term data set from BAO provides a more robust estimate of the CO/CO_2ff ratio than either of these short-term studies where small errors in individual data points could result in a large difference in the estimated ratio and where short term variability could have a strong influence. For comparison with these short term data sets, observed ratios of CO/CO_2ff for individual samples from the south wind sector at BAO range from 3.6 to 13.5 ppb ppm^{-1} (1σ), with a maximum observed value of 20 ppb ppm^{-1} (not including the sample impacted by biomass burning). Differences in the influencing area of emissions between the two studies may also play a role in the observed differences.

The main anthropogenic sources of CO in Colorado, and in much of the US, are from on-road gasoline vehicles in the mobile sector (66 %) and from non-road gasoline-based equipment (26 %) (NEI, 2008). While the on-road and non-road sectors account for 92 % of total CO emissions in Colorado, these sectors contribute only 29 % of the total CO_2ff emissions according to the Vulcan08 data product (Gurney et al., 2009), suggesting that the CO/CO_2ff emission ratio from other combustion sources is very small. Similar CO/CO_2ff ratios for both N/E and S wind sectors, therefore, suggests a similar contribution of on-road and non-road CO_2ff sources in both Weld/Larimer counties and the Denver metro counties, consistent with the Vulcan emissions which estimates that the on-road plus non-road sectors, the dominant CO contributors, combine for 29 % and 41 % of the total CO_2 emissions, for Weld/Larimer and Denver metro respectively (Gurney et al., 2009). This is in contrast to CH_4 and other trace gases, as we discuss below, where there is a clear enhancement due to non-combustion sources related to oil and gas production.

3.2.2 Methane

We find significant differences in the mole fraction of CH_4 relative to CO_2ff depending on wind direction. This can be seen in the correlation plot of CH_4 with CO_2ff (Fig. 3b), where filtering by wind sector results in two highly correlated relationships (r^2 of 0.87 and 0.69 for Weld county and the metro Denver counties, respectively); however, the slope is higher by a factor of 3 in the N/E wind sector relative to the S wind sector. The implication of this is that emissions of CH_4, relative to CO_2ff, are 3 times higher in the N/E sector than the S sector. The added source of methane influencing air samples arriving from the N/E are likely due to fugitive emissions of raw gas and flashing emissions from condensate storage tanks (Pétron et al., 2012). Most of the operations are located in Weld County in the DJB. Condensate tanks store a semi-liquid mix of hydrocarbons separated from raw natural gas; flashing emissions occur when condensate liquids experience a drop in pressure, causing entrained gas to escape. Venting/fugitive emissions can originate at the wellhead and occur when new gas or oil wells are drilled and completed or when existing wells are vented or repaired. Additional sources of methane from the oil and gas sector may include pipeline leaks, pneumatic devices and pumps, and incomplete combustion in compressor engines. Cattle feedlots, wastewater treatment plants, and landfills are also present in the region and likely contribute significantly to the CH_4 signal at BAO.

While venting and flashing are not associated with combustion, except insofar as they are co-located with heavy equipment and compressor engines, there is the possibility of entrained CO_2ff being co-emitted from natural gas wells. CO_2 can be a small fraction (3–5 % by mass) of raw natural gas (COGCC, 2011), but constitutes only a negligible fraction (< 0.1 %) of total Weld/Larimer county CO_2 emissions, based on the estimates of Pétron et al. (2012). This suggests that the correlation of CO_2ff with CH_4 is due primarily to similarly located, but separate processes. Further evidence of this can be found in a consideration of multiple tracer/CO_2ff ratios, as we will discuss below.

3.2.3 Other trace gases

To further understand the differences in emissions between the two wind sectors, we consider the differences across a series of tracer/CO_2ff ratios. Figure 5 shows the difference in median tracer/CO_2ff ratios for CO, C_2H_2, CH_4, C_3–C_5 alkanes, and benzene when winds are from the N/E and from the S. Like CO, C_2H_2 is emitted overwhelmingly from combustion sources, while the other trace gases are emitted either from non-combustion sources (C_3H_8, n-C_4H_{10}, and n-C_5H_{12}) or from a combination of sources. Both CO and C_2H_2 show no appreciable dependence on wind direction, consistent with the idea that both gases are emitted primarily from combustion processes that are common to Weld/Larimer counties and the Denver metro counties. The median enhancement ratio of C_2H_2 to CO_2ff observed at BAO (N/E and S combined) is 43.7 (38.3–55.4) ppt/ppm (16th–84th percentile range) ($r^2 = 0.81$), which is consistent with observations from two previous studies in different locations: 52 (45–59) ppt/ppm downwind of Sacramento, CA (Turnbull et al., 2011) and 45.9 (28.6–102.9) ppt/ppm off the east coast of the United States during winter (Miller et al., 2012). This consistency suggests a relative insensitivity of this ratio to a particular mix of emission type across the United States, an important criterion if one were to consider using C_2H_2 as a proxy for CO_2ff in the absence of $\Delta^{14}CO_2$ observations. However, the large spread observed in the enhancement ratio off the eastern US coast by Miller et al. (2012) (as reflected by the 16th and 84th percentiles of the distribution of observed ratios) suggests that there can be more variability in this ratio than indicated by the range of median values alone. Additional research is required to better evaluate the potential for using C_2H_2 as a secondary CO_2ff tracer and whether it would prove advantageous over the use of CO (Turnbull et al., 2006; Levin and Karstens, 2007), which may [illegible] problematic in locations where significant is situ production results from VOC oxidation.

As with CH_4, there are significant differences in the tracer/CO_2ff enhancement ratios for the C_3–C_5 alkanes and benzene with wind direction, which suggests that enhanced emissions of these chemicals are associated with gas and oil operations (Bar-Ilan et al., 2008a,b; Pétron et al., 2012). In general, ratios of C_3–C_5 alkanes are enhanced relative to CO_2ff by about a factor of 10 in the N/E wind sector compared to the S wind sector. Benzene is enhanced in the N/E wind sector compared to the S wind sector by a factor of 1.6. Despite the significant non-combustion sources of the VOCs related to gas and oil production, we see very good correlations of these species with CO_2ff in air arriving from the N/E ($r^2 > 0.75$), an indication of integration of emissions by air mass mixing or substantial co-location of combustion sources with gas and oil wells and condensate tanks.

3.3 Estimating emission magnitudes

From the observations described above as well as those reported in the CFRPS, it is clear that air sampled at the BAO tall tower is influenced by emissions on local and regional scales. Changes in wind direction at the site result in these local emissions coming from one of two primary source regions: (1) gas and oil operations to the north and east and (2) the Denver metro region to the south. Given the distinct geographical separation of sources, we use the wind sector specific observations, in conjunction with county-level CO_2 emissions from the Vulcan data product (Gurney et al., 2009) as a means to constrain emissions for these trace gases using a top-down approach.

$$E_x = E_{CO_2ff}\left(1 + \alpha/100\right) R \tag{4}$$

Equation (4) describes the annual average top-down emissions for a series of trace gases (E_X), where R is the median observed tracer/CO_2ff ratio, E_{CO_2ff} is the annual average Vulcan CO_2ff emission rate for the region of interest, and α is a scaling factor that is designed to account for changes in emissions from the emission base year to the observation period. For CO_2ff emissions, this factor is equal to the change in emissions (expressed as a %) for the EIA inventory for Colorado state between 2002 (the Vulcan base year) and the most current EIA inventory year, 2009. Equation (4) is applied independently to the N/E and S wind sectors for each tracer, with R calculated for the N/E and S wind sectors paired with E_{CO_2ff} estimates for Weld/Larimer counties and the metro Denver counties, respectively. Since α is based on state wide changes in E_{CO_2ff}, this scaling factor is equivalent for both wind sectors. Tracer/CO_2ff ratios (R) are calculated as discussed in Sect. 3.2. Table 1 summarizes the parameters used to calculate E_X for Weld/Larimer counties and the Denver metro counties. Note that the observation period spans two summers (and one winter) and thus any seasonal bias in the observed value R would lead to summer emissions being over-represented in the estimates of E_x. From the available data, however, we can detect no significant differences (with respect to the 2σ confidence intervals) in R with season for any of the trace gases considered.

Uncertainties in R (as described in Sect. 3.2), $E_{\mathrm{CO_2ff}}$, and α are considered (among other factors) in the estimation of top-down emissions. The scaling term, α, is 2.8 % for the state of Colorado according to the EIA inventory. While this scaling term indicates almost no change between 2002 and 2009 emissions, in actuality, emissions increased by 9 % by 2007 and then decreased over the next 2 yr (presumably related to the economic downturn in the United States during this period). Similar trends are observed in the county level Vulcan emissions over this time period, though the peak year in both Denver Metro and Weld/Larimer counties occurs earlier than 2007. Using changes in the annual EIA-based Colorado emissions to scale the Denver Metro and Weld/Larimer Vulcan02 estimates, gives, in general, very good agreement with the Vulcan estimates for these counties from 2003–2008 (to within 10 % for any given year and about 5 % on average). The Vulcan02 uncertainties (1σ) for the individual counties considered here are of similar order, ranging from 4.6 % to 10.6 % (K. Gurney, unpublished results), with less uncertainty associated with the combined larger county "sectors" that we use in our wind sector analysis. Doubling these uncertainties (to be consistent with our 2σ analysis) for the two wind sectors results in differences from the central estimate of 7 % (upper estimate) and 11 % (lower estimate) for Weld/Larimer counties and 7 % (upper) and 10 % (lower) for the Denver metro counties. We therefore assign a conservative uncertainty of ±20 % to the scaled bottom-up $\mathrm{CO_2}$ff emissions estimates in this analysis, folding in uncertainty in both $E_{\mathrm{CO_2ff}}$ and α.

The calculated top-down estimates (E_x) are given as a central estimate or "best guess" for the annual emissions plus 95 % confidence intervals calculated by propagation of the uncertainties described above. For species having sources that are not necessarily spatially correlated with emissions of $\mathrm{CO_2}$ff (e.g. venting and flashing emissions), it is possible that the top-down emissions estimates are biased in some way. However, it is not possible to predict what direction this bias would be in since it is equally likely for an enhanced $\mathrm{CO_2}$ff sample to arrive at the site with no accompanying trace gas enhancement as it is for the trace gas to be enhanced but not $\mathrm{CO_2}$ff. The boot-strap determination of uncertainties for the enhancement ratio puts a reason-able constraint on the impact of less than perfect correlations between the trace gases and CO_2ff. Figure 6a, b summarizes the top-down estimates and confidence intervals (whiskers), along with the available bottom-up estimates (from multiple sources) and top-down estimates from the CFRPS, for each trace gas species considered.

3.3.1 Spatial considerations

Additional uncertainty in E_{CO_2ff} arises as a result of our simplistic assumptions regarding the geographic footprint (area of emissions) influencing the observations. Obviously, the emissions influencing the observations are not strictly confined to the county boundaries that we have selected, based on the simple wind sector analysis. This matters only to the extent that the spatial distribution of tracer/CO_2ff emission ratios varies between the presumed footprint and the actual footprint. This may be an issue especially for emissions estimates in the N/E wind sector where VOC and CH_4 emissions from the DJB are primarily confined to within Weld County while CO_2 emissions are likely significant over a larger spatial scale. For example, there are significant CO_2 emissions along the I-25 corridor (in Larimer County) to the north of BAO, where there are relatively few active gas wells (see Fig. 1). Whereas CO_2 emissions are significant in both Weld (55 %) and Larimer (45 %) counties (according to Vulcan, 2008), the vast majority (~ 99.8 %) of natural gas and oil production (and associated emissions, presumably) in the two counties is confined to Weld County (COGCC, 2011). Thus, the top-down emissions estimates of the trace gases from oil and gas production will be sensitive to our assumptions about the geospatial scale of the observations, specifically, whether the observations are influenced by emission fluxes only in Weld County or across a larger area that extends into the eastern part of Larimer County or other locations where CO_2ff emissions are significant.

An available constraint on these assumptions is the top-down estimates of CH_4 from the CFRPS (Fig. 6a), where bottom-up estimates of C_3H_8 and CH_4 emissions from condensate tanks were used as a quantitative reference. Since C_3H_8 and CH_4 are strongly correlated at BAO and are emitted from the same processes related to the oil

Title Page
Abstract | Introduction
Conclusions | References
Tables | Figures
◀| | |▶
◀ | ▶
Back | Close
Full Screen / Esc
Printer-friendly Version
Interactive Discussion

and gas industry in the region, and thus distributed similarly in space, the CFRPS top-down estimates are somewhat less sensitive to assumptions about the spatial extent of the observation footprint, even though some uncorrelated sources of CH_4 from cattle feedlots, for example, may be significant. Using the CFRPS top-down CH_4 estimate of 143 (72–271) $Gg\,yr^{-1}$ (which has been scaled up to 2009–2010) and our observed CH_4/CO_2ff ratio of 30 $ppb\,ppm^{-1}$, we calculate corresponding CO_2ff emissions of 3.6 (1.8–6.8) $Tg\,C\,yr^{-1}$. The central estimate of this calculation is about 20 % greater than the Larimer plus Weld county CO_2ff emissions from the scaled Vulcan data product. For Weld County alone, the central estimate (1.7 $Tg\,C\,yr^{-1}$) is just below the lower end of the range of estimates. The range of top-down CH_4 estimates from L12 is considerably lower than the CFRPS estimates, resulting in inferred CO_2ff emissions of 1.1–2.2 $Tg\,C\,yr^{-1}$ (using “realistic errors”) or 1.1–3.3 $Tg\,C\,yr^{-1}$ (using “conservative errors”). The inconsistencies between the CFRPS and L12 are significant, and it is beyond the scope of this study to pass judgment on the validity of one estimate over the other, so we simply expand the range of top-down CO_2ff estimates to be consistent with both studies.

The full range of CO_2ff emissions estimates (1.1–6.8 Tg C), as derived from the CFRPS and L12 top-down CH_4 estimates, is much larger than the 20 % uncertainty that we prescribe for the county-level bottom-up emissions, and thus translates to a large uncertainty in the spatial extent of emissions influencing observations at BAO. We expect that our analysis of trace gas emissions related to the oil and gas industry in the N/E wind sector to be particularly sensitive to the uncertainty in the spatial extent of observations, due to the relatively poor spatial correlation between CO_2ff sources and oil and gas operations across the whole of Weld and Larimer counties. Thus, we use this range of E_{CO_2ff} estimates (1.1–6.8 Tg C) to set the uncertainty limits on our determination of emissions for the trace gases related specifically to the oil and gas industry in Weld County (CH_4, benzene, and the C_3–C_5 alkanes). These upper and lower bounds should be interpreted as representing an upper limit of the uncertainty resulting from having no independent information about the spatial extent of this analysis. Therefore, while this range is large and does not provide an independent estimate of emissions of these trace gases (due to the reliance on CFRPS and L12 calculations), it does allow us to set a conservative range of geospatial scales over which a series bottom-up vs top-down comparisons can be made. We will revisit this discussion in Sect. 3.3.4 by performing a sensitivity test of our top-down analysis to different assumptions about the spatial extent of our observations, using CH_4 as an example. For CO and C_2H_2 and for all emissions estimates for the Denver metro counties we assume that tracer emissions are more spatially correlated with CO_2ff and assign uncertainty as described in Sect. 3.3.

3.3.2 Carbon monoxide

We estimate annual CO emissions to be 65.8 (50.1–81.7) $\mathrm{Gg\,yr^{-1}}$ CO for Weld/Larimer counties and 175.1 (106.8–241.2) $\mathrm{Gg\,yr^{-1}}$ CO for the metro Denver counties. The NEI08 estimates for these regions are 120.1 Gg CO and 362.1 $\mathrm{Gg\,yr^{-1}}$ CO, corresponding to overestimates by a factor of 1.8 and 2.1, for Weld/Larimer and metro Denver counties, respectively (Fig. 6). Total emissions for the two regions are overestimated by a factor of 2.1 in the NEI bottom-up inventory; the range of uncertainty in the combined top-down estimate corresponds to a range of 1.7–2.8 for the overestimate of the NEI bottom-up inventory. These values are consistent with prior studies evaluating the accuracy of the NEI CO emissions (Parrish, 2006; Hudman et al., 2008; Miller et al., 2008, 2012; Turnbull et al., 2011).

Comparing the results of different studies where radiocarbon observations were used to derive CO/CO_2ff ratios provides some insight into the ubiquity of the overestimate of CO emissions in the NEI inventory. A survey of observed CO/CO_2ff ratios from different locations, including Sacramento, CA (Turnbull et al., 2011), Denver (Turnbull et al., 2006; Graven et al., 2009), Irvine, CA (Djuricin et al., 2010), and off the eastern coast of the United States (Miller et al., 2012), reveals regional differences in the agreement between observations and bottom-up estimates (Fig. 4). The observations off of the eastern seaboard of the United States point to an overestimate of NEI CO emissions

(Miller et al., 2012), consistent with the BAO observations and with the numerous literature examples finding CO emissions are over-estimated across the US (Hudman et al., 2004; Parrish, 2006). However, both California-based studies find that the observed CO/CO_2ff ratio closely matches the estimates from California bottom-up inventories (Fig. 4). The Sacramento results were compared with bottom-up estimates from both the California Air Resources Board and NEI05 inventories by Turnbull et al. (2011). The authors of that study found good agreement with the CARB 2008 inventory and a factor of about two overestimate in the NEI05 inventory. From our analysis, it appears as though this overestimate in the NEI inventory for California has been corrected in the 2008 release, perhaps a result of adopting the CARB estimates, as previously suggested by Turnbull et al. (2011). Similarly, the observations in Irvine (Djuricin et al., 2010) are in good agreement with the NEI08 inventory for the LA Basin (Los Angeles, Orange County, San Bernardino, and Riverside counties). From the BAO observations and those off the east coast of the US, it appears as though this correction was not made for the rest of the country.

As with the previous Denver observations, the Sacramento and Irvine observations are representative of shorter time periods: the Sacramento observations were compiled from linear correlations of several samples collected during 2 aircraft flights, while the Irvine observations were from 3 discrete samples collected over a few different months at a surface site on the campus of UC Irvine. The Miller et al. study provides a longer term average, similar to the BAO observations, but is more representative of northeast US regional-scale ($\sim 10^5$–$\sim 10^6$ km^2) sources rather than the local-to-regional ($\sim 10^3$–$\sim 10^5$ km^2) influence at BAO. Given the large differences in scale relevant to each of these studies, the comparisons of CO/CO_2ff ratios in the various locations are not necessarily conclusive. However, as we will discuss in Sect. 4.1, we find that a closer inspection of the NEI08 inventory reveals a significant difference in the CO inventory in California vs Colorado that is not supported by observations.

In situ production or loss of CO could potentially bias these results. The most likely scenario would be the production of CO from the oxidation of VOCs by OH (Griffin et al., 2007) and can be significant in some locations, especially during summer when oxidation rates are intensified and biogenic VOC emissions are high. At BAO, we do not see an appreciable difference in the CO/CO_2ff ratio from winter to summer, which suggests a minimal influence of photochemistry on CO abundance at BAO. The atmospheric lifetime of CO is sufficiently long (~ 50 days) that its impact is negligible to this analysis.

3.3.3 Acetylene

Acetylene emissions are estimated to be 0.28 (0.21–0.40) Gg yr^{-1} in Weld/Larimer counties and 0.78 (0.54–1.0) Gg yr^{-1} in the Denver Metro counties. These values are higher than the bottom-up estimates by factors of 1.5 (1.1–2.1) and 1.4 (0.9–1.7) for Weld/Larimer and Denver metro, respectively (Fig. 6). In contrast to carbon monoxide, there has been very little evaluation of C_2H_2 emissions inventories in the United States. Warneke et al. (2007) compared the C_2H_2 : CO ratio from observations in Boston, New York, and Los Angeles to that in the NEI99 emissions database, and found the ratio to be underestimated in each location, suggesting a systematic underestimation of acetylene emissions by the NEI database. However, it is unclear whether this underestimation of the C_2H_2 : CO ratio is a result of an underestimate of C_2H_2 or an overestimate of CO (as detailed above). With observations of $^{14}CO_2$, the C_2H_2 inventory can be directly evaluated independently of any biases in the CO emissions inventory. There have been two recent examples comparing top-down estimates of C_2H_2 emissions in the United States to bottom-up inventories using $^{14}CO_2$ observations: Miller et al. (2012) estimated C_2H_2 emissions for the entire United States (assuming northeast ratios were nationally representative) and found relative agreement (within 6 %) with the NEI05 C_2H_2 emissions inventory (the same gridded inventory used for comparison in this study and described above); Turnbull et al. (2011) published a comparison of C_2H_2 : CO_2ff ratios from observations of the Sacramento urban plume with that calculated from bottom-up inventories and found a ~ 30 % underestimate of C_2H_2 in the NEI 2005 inventory for Sacramento, CA. Additional $^{14}CO_2$ observations co-located with C_2H_2 in more locations and comparison with contemporaneous NEI values are required to come to any definitive conclusions regarding the accuracy of C_2H_2 emissions in the NEI database. The use of C_2H_2 as a secondary fossil fuel tracer or a proxy for CO_2ff seems promising, however, and given the limited evaluation of C_2H_2 emission sources in the literature, to date, further studies are recommended.

3.3.4 Methane

As discussed in Sect. 3.2.2, we sample different sources of CH_4, as well as benzene and the C_3–C_5 alkanes, relative to CO_2ff emissions with changing wind direction. The oil and gas operations to the northeast of BAO, primarily in Weld County, significantly impact concentrations of these species in air at BAO (Pétron et al., 2012), consistent with our findings here. Additional sources, including cattle feedlots, waste water treatment plants, and landfills are likely also important in this region.

Annual emissions of CH_4 are estimated to be 121(40–272) Gg yr^{-1} and 98 (55–138) Gg yr^{-1}, for Weld/Larimer counties and the Denver Metro counties, respectively. Bottom-up estimates from the CFRPS for the former region are 71 (46–100) Gg yr^{-1}, within the lower uncertainty bracket of our top-down estimate (40 Gg yr^{-1}), but considerably below the central top-down estimate (121 Gg yr^{-1}).

As discussed in Sect. 3.3.1, there is significant uncertainty in the spatial extent of emissions influencing observations at BAO, creating ambiguity when defining the geographic constraints for comparing the top-down and bottom-up estimates. We can explore this issue in a more quantitative way by comparing the top-down and bottom-up estimates across a range of geographic areas, using gridded inventories of CO_2ff and CH_4. To do this we convolve an expanding series of hypothetical footprints or “influence functions” onto the gridded Vulcan02 inventory (0.1° × 0.1°), where an influence function is defined as the sensitivity of an observation at a single point in space to fluxes at any given upwind location. For each hypothetical footprint, we can estimate a different value of E_{CO_2ff} from which a top-down emission rate can be estimated for CH_4 using Eq. (4), with R equal to the observed enhancement ratio. A series of hypothetical footprints is considered that vary in size from 1 × 1 Vulcan grid cells (at 0.1° × 0.1° resolution) to 30 × 30 grid cells and are constructed such that the sensitivity at the receptor to emissions within a given grid-cell decays exponentially with distance from the receptor. Thus the emissions in grid-cells close to the tower are always weighted more heavily than those farther away. These hypothetical footprints are not intended to accurately represent atmospheric transport; rather, they are intended to be used to explore the sensitivity of the top-down vs. bottom-up comparison to spatial assumptions across a range of potential influencing regions. Figure 7a shows the weighted CO_2ff emissions across a footprint (13 × 13 grid cells) extending to the north and east that would give approximate agreement with the top-down CH_4 estimate from the CFRPS (143 Gg yr^{-1}). Figure 7b shows the weighting function used to estimate the emissions in Fig. 7a. From the full series of hypothetical footprints considered, we find that a range of footprints between 4 × 4 Vulcan grid cells and 26 × 26 grid cells are consistent with the full range of CFRPS and L12 top-down CH_4 estimates (72–271 Gg yr^{-1}). This corresponds to an effective area of 2200–74 000 km^2. An analogous series of footprints are generated for the S wind sector, as well.

The same series of footprints are then convolved with the gridded (0.1° × 0.1°) CH_4 inventory (EDGAR) to provide a bottom-up emission rate for comparison with each top-down estimate. The bottom-up emissions are scaled up by 10 % in the N/E wind sector according to changes in oil and gas production between 2008 and 2009–2010 (COGCC, 2011) and by 1.7 % for the S wind sector according to population increases in the Denver metro counties. Figure 8 shows the ratio of bottom-up to top-down CH_4 estimates with changes in the effective footprint size for both the S and N/E wind sector. Uncertainties associated with these calculations are carried through from the 95 % confidence intervals for the top-down estimates, taking into account uncertainties in the observed tracer/CO_2ff ratio, E_{CO_2ff}, and α. To reiterate, these hypothetical footprints are not expected to be an accurate indication of atmospheric transport to the BAO tower, but rather they provide a sense of how sensitive the top-down vs bottom-up comparison is to any presumptions about the geographic region over which emissions are influencing observations at the tower. More directly, this exercise gives an indication of the spatial heterogeneity of CH_4/CO_2ff emission ratios in the bottom up inventory for locations directly upwind of the tower and how this variability influences our conclusions about the accuracy of the bottom-up inventory.

According to the results shown in Fig. 8, the bottom-up/top-down comparison for CH_4 is less sensitive to assumptions about the effective emissions footprint for observations in the S wind sector than in the N/E wind sector. With the exception of only the smallest and largest hypothetical footprints considered, the bottom-up emissions for the S wind sector are always within 7 % of the top-down estimates, and there is general agreement (at > 95 % confidence) with the EDGAR inventory for urban sources across the entire range of hypothetical footprints considered. A footprint extending to the south and east over an area of 30 000 km^2 corresponds roughly to the area over which the CO_2ff emissions are equivalent to that specifically from the Denver metro counties. Over this same area, the EDGAR inventory estimates CH_4 emissions of 99 (98–103) $Gg\,yr^{-1}$ (with the range of estimates reflecting uncertainties in the scaling parameter, α), in very good agreement with the top-down observations. This bottom-up estimate is included in Table 1 and Fig. 6b for completeness.

As discussed above, we estimate that the effective BAO footprint for observations in the N/E wind sector is between 2200 and 74 000 km^2 (or some area of equivalent CO_2 emissions). The estimates in Fig. 8b show that in between the limits set by the uncertainty in the effective footprint size, the EDGAR CH_4 emissions range from 36 %-84 % of the top-down estimates from observations in the N/E wind sector. At the high end of this disagreement, the presumed emissions footprint is sufficiently small (4 × 4 grid cells) that uncertainties in both the CO_2ff and CH_4 gridded inventories are likely high, and a 64 % disagreement is probably not unexpected.

Between 15 000 and 35 000 km^2, the bottom-up estimate is just within or just outside the lower 95 % confidence limit of the top-down estimate. In general, however, the data suggest that emissions of CH_4 are underestimated in the bottom-up inventory. If we remove assumptions about scaling-up the bottom-up inventory from the inventory base year to the observation period, the differences between bottom-up and top-down increase by 10 %. One interpretation of this underestimate could be that additional scaling beyond the prescribed 10 % is required to account for changes in CH_4 emissions from the inventory base year (2008) to the study period, however we show below that this is likely not the only source of error in the bottom-up inventory. Further, it is likely that emissi[illegible] have either decreased or scaled non-linearly with production since 2008 due to state regulations requiring the use of low-bleed pneumatic devices (Sgamma, 2012).

At a footprint size (13 × 13 gridcells) that approximates the Weld/Larimer county-scale top-down estimate, the oil and gas sector in the EDGAR inventory contributes about 30 $\mathrm{Gg\,yr^{-1}}$ (primarily from natural gas systems with a negligible contribution from the oil sector) while the enteric fermentation sector also contributes about 30 $\mathrm{Gg\,yr^{-1}}$. An additional 25 $\mathrm{Gg\,yr^{-1}}$ comes [illegible]m other sources. The implications of this are two-fold: (1) there is potentially an additional 55 Gg of CH_4 emissions annually impacting observations within the N/E wind sector at BAO that are not from the oil and gas industry, and thus, were not considered in the simple two-member mixing model used in the CFRPS or L12; and (2) the 71 $\mathrm{Gg\,yr^{-1}}$ of CH_4 emissions estimated from bottom-up methods for the oil and gas industry in Weld county in the CFRPS are more than double the EDGAR inventory for this sector. This second point suggests that there is a problem with the base year EDGAR inventory and not with the prescribed 10 % scaling term since the base year for both the CFRPS and the EDGAR inventory is 2008. Importantly, neither the EDGAR nor the CFRPS bottom-up inventories are wholly representative of CH_4 emissions in this region. In fact, as shown in Fig. 9, it is found that by combining the sectors not related to the oil and gas industry in the EDGAR inventory with the CFRPS inventory (which includes the oil and gas sector only), the total emissions in the bottom-up inventory are in relative agreement with the top-down observations (∼ 12 % overestimate in the bottom-up). It is worth noting that repeating this analysis for slightly larger or slightly smaller footprints gives consistent results, with bottom-up vs top-down estimates agreeing to within ±10 % when the CFRPS oil and gas emissions are merged with the EDGAR inventory.

In the Denver metro counties the natural gas systems sector contributes about 30–35 % of total CH_4 emissions, which is similar to the contribution of natural gas systems to CH_4 emissions in Weld/Larimer counties. Scaling up the natural gas systems sector in the EDGAR inventory for the Denver metro counties, therefore, would result in a large over estimate of CH_4 emissions. A key difference, however, is the types of sources within the natural gas systems sector contributing to emissions in Denver vs Weld/Larimer. According to statistics about natural gas production in the region (COGCC, 2011), natural gas production in the Denver metro counties is about 4 % of that in Weld county. Thus, emissions to the south and east of BAO likely arise from refineries and/or gas distribution networks from which the EDGAR bottom-up inventory estimates emissions that are consistent with the observations at BAO.

3.3.5 Benzene

Total benzene emissions in Weld/Larimer counties are estimated to be 0.64 (0.22–1.44) $\mathrm{Gg\,yr^{-1}}$ and 0.95 (0.71–1.28) $\mathrm{Gg\,yr^{-1}}$ in the Denver metro counties. Benzene emissions in the NEI08 inventory are 0.49 $\mathrm{Gg\,yr^{-1}}$ for Weld/Larimer counties, at the low end of the observed uncertainty range; the Denver metro emissions are 1.30 $\mathrm{Gg\,yr^{-1}}$, which is just outside the upper limit of the top-down uncertainty range. This suggests that the NEI08 benzene emissions are not inconsistent with the observations at 95 % confidence, but would likely not be in agreement under relaxed confidence criteria. The top-down emissions from the CFRPS (0.39–1.19 $\mathrm{Gg\,yr^{-1}}$) are consistent with our top-down estimates.

Mobile combustion and evaporative sources represent the largest contributor to benzene emissions in the NEI08 inventory in both the Denver metro counties and in Weld/Larimer counties. In the Denver metro counties mobile sector vehicles contribute to 92 % of the benzene emissions, compared with 80 % in Weld/Larimer combined and

50 % in Weld County alone. Therefore, a comparison of top-down estimates to the bottom-up inventories of benzene from Weld County (and not over a larger footprint, as we have determined) may be biased. The CFRPS bottom-up estimate for benzene emissions, which corresponds to venting and flashing emissions in Weld county only, is 0.14 (0.05–0.23) Gg yr^{-1}. This equates to a significant fraction of what the NEI08 estimates for the region: 10–49 % of the total Weld/Larimer benzene NEI08 emissions and 20–90 % of the Weld County NEI08 emissions. According to the NEI08 inventory, the non-combustion sources in the industrial sector, where the venting and flashing emissions would occur, account for only 11 % of the total Weld/Larimer emissions and 20 % of the Weld County emissions. It is likely, then, that the benzene sources of the CFRPS inventory and the NEI08 inventory are mutually exclusive, and a better estimate for Weld/Larimer counties might be the sum of both inventories. The sum of the bottom-up CFRPS and NEI08 estimates for Weld/Larimer counties is 0.54–0.72 Gg yr^{-1}, in better agreement with the top-down estimates (both this study and the CFRPS) than either of the bottom-up inventories alone. Better agreement of the NEI08 benzene emissions with observations for the Denver metro region suggests that the mobile sources are well-accounted for or even slightly over-estimated in the NEI08 inventory.

3.3.6 C_3–C_5 alkanes

Absolute emissions of the 4 studied C_3–C_5 alkanes in Weld/Larimer counties are comparable or greater than those estimated for the Denver metro counties. Propane and *n*-butane exhibit the largest enhancements, with total emissions in Weld County being 2.5 and 2.4 times higher, respectively, than that of the Denver metro counties. Emissions of *iso*-pentane, which is associated with gasoline vehicle emissions (Watson et al., 2001) in addition to oil and gas production (Pétron et al., 2012), are similar in the two regions, and total emissions of *n*-pentane, associated mainly with oil and gas production in the region (Watson et al., 2001; Pétron et al., 2012), are about 1.9 times higher in Weld/Larimer counties.

In the Denver metro counties the bottom-up estimates in the NEI 2005 inventory show a consistent over-estimate for most of the alkanes, relative to the top-down observations. The one exception is propane, which is significantly underestimated (by a factor of ~ 10) in the bottom-up inventory. We see better agreement in Weld/Larimer counties, but the same general relationship in the bottom-up vs top-down comparison: propane is underestimated in the NEI05 inventory relative to the observations (although it is within the lower uncertainty bracket), while the other alkanes are overestimated, but also within the uncertainty brackets. Recent emissions cutting regulations targeting the oil and gas industry in Colorado may explain the overestimate of the alkanes in the NEI05 bottom-up inventory; however, there appears to be a systematic underestimate of propane. There have been similar findings in two other recent studies that utilized $^{14}CO_2$ observations (Turnbull et al., 2011; Miller et al., 2012) to compare top-down and bottom-up estimates of propane.

A chemical sink of the C_3–C_5 alkanes would theoretically lead to an underestimate of emissions by the top-down methods used here, with stronger biases for the larger, shorter-lived alkanes. As detailed in Table 2, the lifetimes of these alkanes range from 3 days, for the pentanes, to 5 days for *n*-butane, to 12 days, for propane. There was some evidence in the CFRPS for OH chemistry influencing the ratios of various alkane tracers when measured close to sources vs at BAO (Pétron et al., 2012). In the east coast study of Miller et al. (2012), which used off-shore sampling sites well removed from local sources, summertime tracer/CO_2ff ratios were lower than wintertime ones, in proportion to their chemical lifetime with respect to OH. We find only minor differences (which are well within the uncertainties), however, in the relative ratios of alkanes with CO_2ff from summer to winter, so we use year-round observations in the current analysis. The seasonal impacts of photochemistry are likely minimized somewhat by subtracting a seasonally variable and relatively nearby background prior to calculating the enhancement ratios. For some perspective, an 8 h atmospheric residence time at an average OH molecular density of 5×10^6 cm^{-3} would result in an underestimate of about 10 Gg yr^{-1} in the C_3H_8 emissions estimate, which is well within the uncertainty brackets of the top-down estimate of 14–64 Gg yr^{-1}. Thus, while we cannot rule out the influence of OH chemistry, we assume that any chemical effects are small relative to other sources of uncertainty in the analysis.

4 Implications for carbon monoxide and methane inventories

Observations of $\Delta^{14}CO_2$ at the BAO tower have provided an important tracer with which to better constrain and evaluate emissions of a suite of compounds important to climate and air quality related to combustion and industrial processes along the northern Colorado Front Range. In this section, we will discuss important implications of our findings related to our evaluation of bottom-up inventories of carbon monoxide and methane, two globally important atmospheric trace gases.

4.1 Carbon monoxide bottom-up inventory

As discussed in Sect. 3.3.2, our observations and evaluation of the NEI08 inventory are consistent with prior findings that CO emissions are overestimated at the national level in previous versions of the (Parrish, 2006; Hudman et al., 2008; Miller et al., 2008). There is evidence, albeit from a limited number of samples, that the California county-level bottom-up emissions of CO more accurately reflect the emissions estimated from atmospheric observations (Fig. 4). This provides the motivation to investigate whether there are fundamental differences in the methods for compiling the bottom-up CO inventory in California vs Colorado, as well as in other states.

An analysis of the on-road sector CO (NEI08) and CO_2ff (Vulcan08) emissions in comparison with the on-road observations of tail-pipe emissions of CO by Bishop and Stedman (2008) in Denver and Los Angeles suggests that NEI08 CO emissions in the on-road sector, specifically, are biased high in Colorado. Their observations show only very small differences between the CO-to-fuel-burnt ratio (and therefore the CO/CO_2 ratio) emitted from vehicles in Denver (in 2006) and Los Angeles (in 2008). The CO-to-fuel-burnt ratios observed in the two cities correspond to CO/CO_2 emission ratios of 16 ppb ppm^{-1} (Denver in 2006) and 18 ppb ppm^{-1} (Los Angeles in 2006). In Los Angeles, the observed ratio (Bishop and Stedman, 2008) closely resembles the bottom-up ratio of 17 ppb ppm^{-1} calculated from the NEI08 and Vulcan inventories for the on-road sector only; however, the on-road sector bottom-up ratio for Denver is 40 ppb ppm^{-1}, 2.5 times the observed ratio. Similarly, in Weld/Larimer counties the bottom-up ratio is 43 ppb ppm^{-1} and US-wide it is 38 ppb ppm^{-1}. It should be noted that the on-road CO emissions in California are estimated using a different mobile source model, EMFAC2007 (EMFAC, hereafter) (CARB, 2007) than what is used for the rest of the United States, MOBILE6.2 (MOBILE, hereafter) (EPA, 2012a). In light of our comparison of CO/CO_2ff observations between California and other regions, and given the Bishop and Stedman (2008) observations in comparison with the on-road sector bottom up inventories, it appears likely that the MOBILE CO emission factor outputs are biased high relative to the EMFAC model.

This is also consistent with a recent comparison (Fujita et al., 2012) of these two mobile source models, along with the MOVES2010a (MOVES, hereafter) model, which was recently adopted by the EPA (EPA, 2010). This study showed that MOBILE emission factor outputs are biased high relative to the EMFAC and MOVES outputs, both of which showed close agreement with observations in a Los Angeles tunnel. This analysis showed that CO was over-estimated by the MOBILE model by a factor of 1.6–2.0 across a range of temperatures and traffic conditions and was found to be relatively insensitive to whether emission control programs were included in the model inputs. Both EMFAC and MOBILE use a region-wide average driving schedule and speed to compile emission factors for different vehicle types and model years, while MOVES uses a more specific approach, where emission factors are calculated for different speed and power bins. The consistency between MOVES, EMFAC, and the observations detailed in Fujita et al. (2012), suggests that the general framework of the MOBILE model for scaling up emission factors from individual vehicles for an average driving schedule, which is essentially the same as that used by the EMFAC model, is not the issue.

Rather, the emission ratios associated with individual vehicle types and model years needs to be adjusted. A separate study by the Federal Highway Administration Resource Center (Claggett and Houk, 2008) also analyzed differences in emission factor outputs by the EMFAC and MOBILE models and found that across a spectrum of average vehicle speeds for identical vehicle fleets in 2010 (a future scenario in the 2008 study), the MOBILE model CO emission factors were higher than the EMFAC output by 50 %–300 %, depending on the average vehicle speed. More recently, a study comparing CO and NO_x observations in Ada County, Idaho with outputs from both MOBILE and MOVES found differences in the CO/NO_x ratio outputs from the two source models, though most of the differences were attributed to differences in NO_x, not CO (Wallace et al., 2012).

With the EPA soon to adopt MOVES2010a for the NEI, and given the analysis of Fujita et al. (2012), future releases of the NEI inventory are predicted to produce more accurate estimates of CO emissions for Colorado and the rest of the US However, continued evaluations of these mobile source models should be performed alongside observations such as those presented here, as well as those from Bishop and Stedman (2008) and Fujita et al. (2012).

We derive a modified bottom-up CO estimate for the Denver metro counties and Weld/Larimer counties in which the NEI08 on-road sector CO emission rate is replaced with a new estimate calculated from the Vulcan08 on-road sector CO_2 emission rate and the observed on-road sector CO/CO_2 ratio of 16 ppb ppm^{-1} from Bishop and Stedman (2008). This new estimate, shown in Fig. 6 and labeled as “Modified NEI”, brings the top-down and bottom-up values to within 30 % for the Denver metro counties and to within 10 % for Weld/Larimer counties. The remaining discrepancy between these modified estimates and the observations could be a result of some combination of: (1) diesel vehicles that contribute significantly to the on-road sector CO_2 emissions but are not a significant source of CO; and (2) a reduction in the CO-to-fuel-burnt emission ratio between 2008 and 2009–2010. Additionally, this crude scaling exercise does not take into account changes in the CO/CO_2 emission ratio during “cold starts”, which likely introduces significant variability at smaller spatial scales and shorter temporal scales. With these caveats acknowledged, scaling-up of this modified CO inventory reduces the total anthropogenic source of CO in the United States from 60 Tg yr^{-1} to 39 Tg yr^{-1}, close to the 60 % reduction recommended by Hudman et al. (2008) for anthropogenic CO emissions in the United States and close to the national $^{14}CO_2$ based estimate of 41 (33–53) Tg yr^{-1} (Miller et al., 2012).

4.2 Methane from oil and gas production

The findings of the CFRPS suggested the presence of enhanced CH_4 levels at BAO over that predicted by bottom up statistical data on condensate tanks and raw natural gas profiles within the Denver Julesberg Basin (Pétron et al., 2012). These findings have since been scrutinized for not considering agricultural sources of CH_4 (Sgamma, 2012) and for the methodology of using methane-to-propane ratios to derive its top-down estimates (Levi, 2012). The results presented here bring a new perspective to this problem, and we arrive at conclusions that are largely independent of the assumptions and methodology used in the CFRPS and in L12. From our analysis of the EDGARv4.2 CH4 emissions estimates for the region, we find that the top-down methodologies in both the L12 and CFRPS studies are flawed in that they fail to consider additional sources of CH_4 that are not directly related to the oil and gas industry in the region. We find that the bottom-up CH_4 emission estimate derived in the CFRPS is not inconsistent with the top-down estimates using observations at the BAO tower, but that additional sources, primarily enteric fermentation, must be also considered. In these previous studies the contribution from other sources to the CH_4 signal at BAO has resulted in either an overestimate of the venting/fugitive CH_4 source (CFRPS) or a larger methane-to-propane ratio for raw natural gas than is likely to be present in the region (L12).

Natural gas systems are a large source of CH_4 on continental and global scales according to the EDGAR inventory and others (e.g. EPA, 2012b). A comparison of the CFRPS bottom-up estimate and the oil and gas systems sector in the EDGARv4.2 inventory suggests that an additional ~ 40 Gg yr^{-1} are missing from the EDGAR inventory for the region. This equates to an underestimate of about 60 % for the oil and gas sector within the EDGAR inventory, on a local scale. One explanation for this underestimate could be an error in the spatial allocation of CH_4 emissions, such that emissions are estimated accurately over larger spatial scales but local inaccuracies arise when geographically distributing the emissions. Thus, it is impossible to speculate on whether this underestimate is systematic across the oil and gas sector in the EDGAR inventory; however, it should be noted that, in theory, this underestimate would scale up to a significant underestimate (~ 30 %) of total CH_4 emissions across the United States. More observations are recommended, therefore, across a range of spatial and temporal scales in different regions to properly evaluate EDGAR, and other CH_4 emission databases, in the context of continental or global scale emissions, which could have potential implications for global atmospheric chemistry and climate. Our results provide strong motivation for the continued use of $^{14}CO_2$ observations in these evaluations.

5 Summary and conclusions

We have analyzed 145 whole air samples for $\Delta^{14}CO_2$ collected across 15 months at the NOAA BAO tall tower in Erie, Colorado. Air sampled at this site is heavily impacted by emissions from a variety of local sources including urban, rural, and industrial activities. The oil and gas industry, in particular, was found to contribute to enhancements in a number of industry-related trace gases relative to fossil fuel CO_2 when the tower is downwind of oil and gas activities, which are concentrated in Weld County to the north and east. The observed enhancements suggest that CH_4, C_3–C_5 alkanes, and benzene emissions (relative to CO_2ff emissions) are a factor of 3, ~ 10, and 1.6 greater, respectively, in air masses arriving passing over Weld and Larimer counties (north and east) over those originating from the Denver metro counties (south).

With the availability of a spatially resolved bottom-up CO_2ff emissions data product from the Vulcan Project, we are able to take advantage of correlations of various trace gases with CO_2ff, derived from $\Delta^{14}CO_2$ observations, in order to critically evaluate the accuracy of the bottom-up emissions inventories of these gases. The primary source of uncertainty in this approach is the uncertainty in the spatial extent of the observation footprint, and therefore the precise reference emissions value for CO_2ff. This is particularly relevant for Weld and Larimer counties, which presents an extreme case where emissions related to the oil and gas industry are confined to a well-defined region within a larger region of significant CO_2ff emissions from mobile sources and there is significant spatial heterogeneity in tracer/CO_2ff emission ratios. Observations of trace gases alongside $^{14}CO_2$ observations on a mobile platform throughout the N/E sector (i.e. the sampling approach used in the CFRPS) would help to resolve this issue, as would the incorporation of an atmospheric transport model such as STILT (Lin et al., 2003) into the analysis. We find that our results for the Denver metro counties are less sensitive to assumptions regarding the spatial extent of the observation footprint, at least for CH_4. Within the constraints set by this and other sources of uncertainty, we conclude that our top-down estimates are inconsistent with the bottom up inventories for CH_4, CO, benzene, and propane.

CO is underestimated in the NEI08 inventory in both Weld/Larimer counties and the Denver metro counties by a factor of ~2, consistent with prior evaluations of earlier NEI inventories in the US over larger scales. From the NEI08 CO and Vulcan08 CO_2ff emissions estimates, we calculate that the average emission factor from on-road gasoline vehicles is ~40 ppb CO ppm^{-1} CO_2 for the region, while our observations are more consistent with an emission ratio of 16 ppb ppm^{-1} for these vehicles.

For Weld/Larimer counties, we find that emissions of benzene and CH_4 are underestimated in the CFRPS bottom-up inventory, but that this underestimate can be explained by considering the contribution of emissions from other sectors (not related to the oil and gas industry) to the signal of these gases at the BAO. We conclude, therefore, that the CFRPS bottom-up CH_4 and benzene estimates are not inconsistent with top-down estimates from BAO, in contrast to the findings of Pétron et al. (2012). Our analysis of the CFRPS and other bottom-up emission estimates suggest that in Weld/Larimer counties the on-road sector contributes to about 75–80 % of benzene emissions, enteric fermentation (e.g. cattle feedlots) contributes about 25 % of CH_4 emissions, and other sources account for an additional 20 % of CH_4 emissions. These results are consistent with 1.7 % of total natural gas production in the DJB being vented to the atmosphere, lower than the range of 2.3–7.7 % estimated by Pétron et al. (2012). Future studies of the impact of the oil and gas industry on atmospheric composition using observations at BAO need to consider these additional emission sources. Additional observations of $^{14}CO_2$ and CH_4 in other oil and gas producing regions and comparisons to bottom-up inventories are recommended to determine whether these results are specific to the DJB or if they are more general.

Acknowledgements. The authors would like to acknowledge Paula Zermeño (CAMS), Shane Bradshaw (CAMS), and Chad Wolak (INSTAAR) for their contributions to $^{14}CO_2$ sample preparation. Funding was provided by DOE's Office of Biological and Environmental Research and NOAA. A portion of this work was performed under the auspices of the US Department of Energy by Lawrence Livermore National Laboratory under Contract DE-AC52-07NA27344.

References

Andrews, A. E., Kofler, J. D., Trudeau, M. E., Williams, J. C., Neff, D. H., Masaire, K. A., Chao, D. Y., Kitzis, D. R., Novelli, P. C., Zhao, C. L., Dlugokencky, E. J., Lang, P. M., Crotwell, M. J., Fischer, M. L., Parker, M. J., Lee, J. T., Baumann, D. D., Desai, A. R., Stanier, C. O., de Wekker, S. F. J., Wolfe, D. E., Munger, J. W., and Tans, P. P.: CO2, CO and CH4 Measurements 1 from the NOAA Earth System Research Laboratory's Tall Tower Greenhouse Gas Observing Network: Instrumentation, Uncertainty Analysis and Recommendations for Future High-Accuracy Greenhouse Gas Monitoring Efforts Atmos. Meas. Technol. Discuss., submitted, 2013.

Atkinson, R., Baulch, D. L., Cox, R. A., Crowley, J. N., Hampson, R. F., Hynes, R. G., Jenkin, M. E., Rossi, M. J., Troe, J., and IUPAC Subcommittee: Evaluated kinetic and photochemical data for atmospheric chemistry: Volume II – gas phase reactions of organic species, Atmos. Chem. Phys., 6, 3625–4055, doi:10.5194/acp-6-3625-2006, 2006.

Bishop, G. A. and Stedman, D. H.: A decade of on-road emissions measurements, Environ. Sci. Technol., 42, 1651–1656, 2008.

Brennan, P. J.: Los Angeles Wildfire Sends Pollution as Far as Denver, Bloomberg, available at: http://www.bloomberg.com/apps/news?pid=newsarchive{\&}sid=aJrSkTFs1dL4, last access: 7 March 2012, 2009.

California Air Resources Board Mobile Sources Emissions Inventory, available at: http://www.arb.ca.gov/msei/onroad/latest{_}version.htm, last access: 10 October, 2007.

Claggett, M. and Houk, J.: Comparing MOBILES6.2 and Emfac2007 Emission Factors, Transp. Res. Record, 2058, 51–57, doi:10.3141/2058-07, 2008.

Colorado Oil and Gas Information System, available at: http://cogcc.state.co.us, (last access: 14 June 2011), 2011.

Conway, T. J., Tans, P. P., Waterman, L. S., and Thoning, K. W.: Evidence for Interannual Variability of the Carbon-Cycle from the National-Oceanic-and-Atmospheric-Administration Climate-Monitoring-and-Diagnostics-Laboratory Global-Air-Sampling-Network, J. Geophys. Res. Atmos., 99, 22831–22855, 1994.

Currie, K. I., Brailsford, G., Nichol, S., Gomez, A., Sparks, R., Lassey, K. R., and Riedel, K.: Tropospheric (CO_2)-C_{14} at Wellington, New Zealand: the world's longest record, Biogeochem., 104, 5–22, 2011.

Djuricin, S., Pataki, D. E., and Xu, X. M.: A comparison of tracer methods for quantifying CO_2 sources in an urban region, J. Geophys. Res.-Atmos., 115, D11303, doi:10.1029/2009JD012236, 2010.

Dlugokencky, E. J., Steele, L. P., Lang, P. M., and Masarie, K. A.: The growth-rate and distribution of atmospheric methane, J. Geophys. Res. Atmos., 99, 17021–17043, 1994.

US Energy Information Administration CO2 Emissions Data, available at: http://www.eia.gov/environment/data.cfm{#}summary, last access: 18 June 2012, 2012.

EPA: Official release of the MOVES2010 motor vehicle emissions model for emission inventories in SIPs and tranportation conformity., Fed. Regist., 75, 9411–9414, 2010.

EPA Speciate Software Download Site: available at: http://www.epa.gov/ttnchie1/software/speciate/, last access: 19 June, 2011.

MOBILE6 Vehicle Emission Modeling Software, available at: http://www.epa.gov/oms/m6.htm, last access: 10 October, 2012a.

EPA: Inventory of U. S. Greenhouse Gas Emissions and Sinks: 1990–2010, available at: http://www.epa.gov/climatechange/Downloads/ghgemissions/US-GHG-Inventory-2012-Main-Text.pdf, last access: 11 September, 2012, 2012b.

Fujita, E. M., Campbell, D. E., Zielinska, B., Chow, J. C., Lindhjem, C. E., DenBleyker, G. A., Bishop, G. A., Schuchmann, B. G., Stedman, D. H., and Lawson, D. R.: Comparison of the MOVES2010a, MOBILE6.2, and EMFAC2007 mobile source emission models with on-road traffic tunnel and remote sensing measurements, J. Air Waste Mgmt. Assoc., 62, 1134–1149, doi:10.1080/10962247.2012.699016, 2012.

Godwin, H.: Half-life of radiocarbon, Nature, 195, p. 984, 1962.

Graven, H. D., Guilderson, T. P., and Keeling, R. F.: Methods for high-precision C_{14} AMS measurement of atmospheric CO_2 at LLNL, Radiocarbon, 49, 349–356, 2007.

Graven, H. D., Stephens, B. B., Guilderson, T. P., Campos, T. L., Schimel, D. S., Campbell, J. E., and Keeling, R. F.: Vertical profiles of biospheric and fossil fuel-derived CO_2 and fossil fuel CO_2 : CO ratios from airborne measurements of Delta(14)C, CO_2 and CO above Colorado, USA, Tellus B, 61, 536–546, 2009.

Graven, H. D. and Gruber, N.: Continental-scale enrichment of atmospheric $^{14}CO_2$ from the nuclear power industry: potential impact on the estimation of fossil fuel-derived CO_2, Atmos. Chem. Phys., 11, 12339–12349, doi:10.5194/acp-11-12339-2011, 2011.

Graven, H. D., Guilderson, T. P., and Keeling, R. F.: Observations of radiocarbon in CO_2 at seven global sampling sites in the Scripps flask network: analysis of spatial gradients and seasonal cycles J. Geophys. Res., 117, D02303, doi:10.1029/2011JD016535, 2012a.

Graven, H. D., Guilderson, T. P., and Keeling, R. F.: Observations of radiocarbon in CO_2 at La Jolla, California, USA 1992–2007: Analysis of the long-term trend, J. Geophys. Res., 117, D02302, doi:10.1029/2011JD016533, 2012b.

Griffin, R. J., Chen, J. J., Carmody, K., Vutukuru, S., and Dabdub, D.: Contribution of gas phase oxidation of volatile organic compounds to atmospheric carbon monoxide levels in two areas of the United States, J. Geophys. Res.-Atmos., 112, D10S17, doi:10.1029/2006jd007602, 2007.

Gurney, K. R., Mendoza, D. L., Zhou, Y. Y., Fischer, M. L., Miller, C. C., Geethakumar, S., and Du Can, S. D.: High Resolution Fossil Fuel Combustion CO_2 Emission Fluxes for the United States, Environ. Sci. Technol., 43, 5535–5541, 2009.

Gurney, K. R., Chandrasekaran, V., Mendoza, D. L., and Geethakumar, S.: Quantification of Uncertainty Associated with NACP high Resolution Fossil Fuel CO_2 Emissions: Updates, Challenges and Future Plans, North American Carbon Program All-Inverstigators Meeting, New Orleans, LA, USA, 2011.

Hsueh, D. Y., Krakauer, N. Y., Randerson, J. T., Xu, X. M., Trumbore, S. E., and Southon, J. R.: Regional patterns of radiocarbon and fossil fuel-derived CO_2 in surface air across North America, Geophys. Res. Lett., 34, L02816, doi:10.1029/2006GL027032, 2007.

Hudman, R. C., Jacob, D. J., Cooper, O. R., Evans, M. J., Heald, C. L., Park, R. J., Fehsenfeld, F., Flocke, F., Holloway, J., Hubler, G., Kita, K., Koike, M., Kondo, Y., Neuman, A., Nowak, J., Oltmans, S., Parrish, D., Roberts, J. M., and Ryerson, T.: Ozone production in transpacific Asian pollution plumes and implications for ozone air quality in California, J. Geophys. Res., 109, D23S10, doi:10.1029/2004JD004974, 2004.

Hudman, R. C., Murray, L. T., Jacob, D. J., Millet, D. B., Turquety, S., Wu, S., Blake, D. R., Goldstein, A. H., Holloway, J., and Sachse, G. W.: Biogenic versus anthropogenic sources of CO in the United States, Geophys. Res. Lett., 35, L04801, doi:10.1029/2007GL032393, 2008.

Lee, B. H., Munger, J. W., Wofsy, S. C., and Goldstein, A. H.: Anthropogenic emissions of nonmethane hydrocarbons in the northeastern United States: Measured seasonal variations from 1992–1996 and 1999–2001, J. Geophys. Res.-Atmos., 111, D20307, doi:10.1029/2005JD006172, 2006.

Lehman, S. J., Miller, J. B., Wolak, C., Southon, J., Tans, P. P., Montzka, S. A., Sweeney, C., Andrews, A., LaFranchi, B. W., Guilderson, T. P., Fischer, M. L., and Turnbull, J. C.: Allocation of terrestrial carbon sources using $^{14}CO_2$; measurement and modeling, Radiocarbon, submitted, 2012.

Levi, M. A.: Comment on "Hydrocarbon emissions characterization in the Colorado Front Range: A pilot study" by Gabrielle Petron et al., J. Geophys. Res.-Atmos., 117, D21203, doi:10.1029/2012JD017686, 2012.

Levin, I. and Karstens, U. T. E.: Inferring high-resolution fossil fuel CO_2 records at continental sites from combined $^{14}CO_2$ and CO observations, Tellus B, 59, 245–250, doi:10.1111/j.1600-0889.2006.00244.x, 2007.

Levin, I. and Kromer, B.: The tropospheric (CO_2)-C-14 level in mid-latitudes of the Northern Hemisphere (1959–2003), Radiocarbon, 46, 1261–1272, 2004.

Levin, I., Kromer, B., Schmidt, M., and Sartorius, H.: A novel approach for independent budgeting of fossil fuel CO_2 over Europe by (CO_2)–C_{14} observations, Geophys. Res. Lett., 30, 2194, doi:10.1029/2003GL018477, 2003.

Levin, I., Naegler, T., Kromer, B., Diehl, M., Francey, R. J., Gomez-Pelaez, A. J., Steele, L. P., Wagenbach, D., Weller, R., and Worthy, D. E.: Observations and modelling of the global distribution and long-term trend of atmospheric $^{14}CO_2$, Tellus B, 62, 26–46, 2010.

Lin, J. C., Gerbig, C., Wofsy, S. C., Andrews, A. E., Daube, B. C., Davis, K. J., and Grainger, C. A.: A near-field tool for simulating the upstream influence of atmospheric observations: the stochastic time-inverted Lagrangian transport (STILT) model, J. Geophys. Res. Atmos., 108, 4493, doi:10.1029/2002JD003161, 2003.

Miller, J. B., Lehman, S. J., Montzka, S. A., Sweeney, C., Miller, B. R., Wolak, C., Dlugokencky, E. J., Southon, J., Turnbull, J. C., and Tans, P. P.: Linking emissions of fossil fuel CO_2 and other anthropogenic trace gases using atmospheric $^{14}CO_2$, J. Geophys. Res. Atmos., 117, D08302, doi:10.1029/2011JD017048, 2012.

Miller, S. M., Matross, D. M., Andrews, A. E., Millet, D. B., Longo, M., Gottlieb, E. W., Hirsch, A. I., Gerbig, C., Lin, J. C., Daube, B. C., Hudman, R. C., Dias, P. L. S., Chow, V. Y., and Wofsy, S. C.: Sources of carbon monoxide and formaldehyde in North America determined from high-resolution atmospheric data, Atmos. Chem. Phys., 8, 7673–7696, doi:10.5194/acp-8-7673-2008, 2008.

Montzka, S. A., Myers, R. C., Butler, J. H., Elkins, J. W., and Cummings, S. O.: Global tropospheric distribution and calibration scale of Hcfc-22, Geophys. Res. Lett., 20, 703–706, 1993.

Muller, S. A., Joos, F., Plattner, G. K., Edwards, N. R., and Stocker, T. F.: Modeled natural and excess radiocarbon: Sensitivities to the gas exchange formulation and ocean transport strength, Global Biogeochem. Cy., 22, GB3011, doi:10.1029/2007GB003065, 2008.

Chemical Kinetics and Photochemical Data for Use in Atmospheric Studies Evaluation Number 15, available at: http://jpldataeval.jpl.nasa.gov/, (last access: 28 June 2010), 2006.

National Emissions Inventory, available at: http://www.epa.gov/ttn/chief/eiinformation.html (last access: 26 January 2011), 2008.

Novelli, P. C., Connors, V. S., Reichle, H. G., Anderson, B. E., Brenninkmeijer, C. A. M., Brunke, E. G., Doddridge, B. G., Kirchhoff, V. W. J. H., Lam, K. S., Masarie, K. A., Matsuo, T., Parrish, D. D., Scheel, H. E., and Steele, L. P.: An internally consistent set of globally distributed atmospheric carbon monoxide mixing ratios developed using results from an intercomparison of measurements, J. Geophys. Res. Atmos., 103, 19285–19293, 1998.

Parrish, D. D.: Critical evaluation of US on-road vehicle emission inventories, Atmos. Environ., 40, 2288–2300, 2006.

Pétron, G., Frost, G., Hirsch, A. I., Montzka, S. A., Karion, A., Miller, B. R., Trainer, M., Sweeney, C., Andrews, A. E., Miller, L., Kofler, J., Ryerson, T., Patrick, L., Siso, C., Kolodzey, W., Lang, P., Dlugokencky, E., Conway, T., Novelli, P., Masarie, K., Hall, B., Guenther, D., Kitzis, D., Miller, J. B., Neff, W., Wolfe, D., and Tans, P. P.: Hydrocarbon emissions characterization in the Colorado front range – a pilot study, J. Geophys. Res. Atmos., 117, D04304 doi:10.1029/2011JD016360, 2012.

Schuur, E. A. G., Trumbore, S. E., Mack, M. C., and Harden, J. W.: Isotopic composition of carbon dioxide from a boreal forest fire: Inferring carbon loss from measurements and modeling, Global Biogeochem. Cy., 17, 1001, doi:10.1029/2001GB001840, 2003.

Sgamma, K. M.: Fracking: Colorado methane study not clear-cut, Nature, 483, 407–407, doi:10.1038/483407e, 2012.

Colorado – Active Gas and Oil Wells – April 2008, avaiable at: http://skytruth.mediatools.org/node/9590, last access: 1 October, 2008.

Stuiver, M. and Polach, H. A.: Reporting of C-14 data – discussion, Radiocarbon, 19, 355–363, 1977.

Suess, H. E.: Radiocarbon concentration in modern wood, Science, 122, 415–417, 1955.

Sweeney, C., Gloor, E., Jacobson, A. R., Key, R. M., McKinley, G., Sarmiento, J. L., and Wanninkhof, R.: Constraining global air-sea gas exchange for CO_2 with recent bomb ^{14}C measurements, Global Biogeochem. Cy., 21, GB2015, doi:10.1029/2006GB002784, 2007.

Thompson, M. V. and Randerson, J. T.: Impulse response functions of terrestrial carbon cycle models: method and application, Glob. Change Biol., 5, 371–394, 1999.

Thoning, K. W., Tans, P. P., and Komhyr, W. D.: Atmospheric Carbon-Dioxide at Mauna Loa Observatory. 2. Analysis of the NOAA GMCC Data, 1974–1985, J. Geophys. Res. Atmos., 94, 8549–8565, 1989.

Turnbull, J., Rayner, P., Miller, J., Naegler, T., Ciais, P., and Cozic, A.: On the use of $^{14}CO_2$ as a tracer for fossil fuel CO_2: quantifying uncertainties using an atmospheric transport model, J. Geophys. Res. Atmos., 114, D22302, doi:10.1029/2009JD012308, 2009.

Turnbull, J. C., Miller, J. B., Lehman, S. J., Tans, P. P., Sparks, R. J., and Southon, J.: Comparison of (CO_2)-C-14, CO, and SF6 as tracers for recently added fossil fuel CO_2 in the atmosphere and implications for biological CO_2 exchange, Geophys. Res. Lett., 33, L01817, doi:10.1029/2005GL024213, 2006.

Turnbull, J. C., Lehman, S. J., Miller, J. B., Sparks, R. J., Southon, J. R., and Tans, P. P.: A new high precision $^{14}CO_2$ time series for North American continental air, J. Geophys. Res. Atmos., 112, D11310, doi:10.1029/2006JD008184, 2007.

Turnbull, J. C., Lehman, S. J., Morgan, S., and Wolak, C.: A New Automated Extraction System for ^{14}C Measurement for Atmospheric CO_2, Radiocarbon, 52, 1261–1269, 2010.

Turnbull, J. C., Karion, A., Fischer, M. L., Faloona, I., Guilderson, T., Lehman, S. J., Miller, B. R., Miller, J. B., Montzka, S., Sherwood, T., Saripalli, S., Sweeney, C., and Tans, P. P.: Assessment of fossil fuel carbon dioxide and other anthropogenic trace gas emissions from airborne measurements over Sacramento, California in spring 2009, Atmos. Chem. Phys., 11, 705–721, doi:10.5194/acp-11-705-2011, 2011.

Van der Laan, S., Karstens, U., Neubert, R. E. M., Van der Laan-Luijkx, I. T., and Meijer, H. A. J.: Observation-based estimates of fossil fuel-derived CO_2 emissions in the Netherlands using Delta ^{14}C, CO and ^{222}Radon, Tellus B, 62, 389–402, 2010.

Vaughn, B. H., Miller, J. B., Ferretti, D. F., and White, J. C.: Stable isotope measurements of atmospheric CO_2 and CH_4, in: Handbook of Stable Isotope Analytical Techniques, edited by: de Groot, P., Elsevier Inc., San Diego, CA, 272–304, 2004.

Vay, S. A., Choi, Y., Vadrevu, K. P., Blake, D. R., Tyler, S. C., Wisthaler, A., Hecobian, A., Kondo, Y., Diskin, G. S., Sachse, G. W., Woo, J. H., Weinheimer, A. J., Burkhart, J. F., Stohl, A., and Wennberg, P. O.: Patterns of CO_2 and radiocarbon across high northern latitudes during International Polar Year 2008, J. Geophys. Res. Atmos., 116, D14301, doi:10.1029/2011JD015643, 2011.

Wallace, H. W., Jobson, B. T., Erickson, M. H., McCoskey, J. K., VanReken, T. M., Lamb, B. K., Vaughan, J. K., Hardy, R. J., Cole, J. L., Strachan, S. M., and Zhang, W.: Comparison of wintertime CO to NO_x ratios to MOVES and MOBILE6.2 on-road emissions inventories, Atmos. Environ., 63, 289–297, doi:10.1016/j.atmosenv.2012.08.062, 2012.

Warneke, C., McKeen, S. A., de Gouw, J. A., Goldan, P. D., Kuster, W. C., Holloway, J. S., Williams, E. J., Lerner, B. M., Parrish, D. D., Trainer, M., Fehsenfeld, F. C., Kato, S., Atlas, E. L., Baker, A., and Blake, D. R.: Determination of urban volatile organic compound emission ratios and comparison with an emissions database, J. Geophys. Res.-Atmos., 112, D10S47, doi:10.1029/2006JD007930, 2007.

Watson, J. G., Chow, J. C., and Fujita, E. M.: Review of volatile organic compound source apportionment by chemical mass balance, Atmos. Environ., 35, 1567–1584, 2001.

Zondervan, A. and Meijer, H. A. J.: Isotopic characterisation of CO_2 sources during regional pollution events using isotopic and radiocarbon analysis, Tellus B, 48, 601–612, 1996.

Table 1. Summary of top-down and bottom-up annual emissions for each tracer discussed in our analysis. Included in this table are: correlation coefficients for each tracer with CO_2ff, observed tracer/CO_2ff ratios, bottom-up emissions directly from each inventory and also scaled to the observation period, and estimated top-down emissions. Bottom-up emissions for CO_2ff are also summarized. Uncertainties on the scaled bottom-up emissions and the top-down emissions are described in Sect. 3.3 and Sect. 3.3.1. Top-down emissions for CO_2ff for the N/E wind sector are estimated using the top-down CH_4 estimates from the CFRPS and L12 as a quantitative reference, as described in Sect. 3.3.1. Bottom-up CH_4 estimates for the S wind sector are detailed in Fig. 8 and associated text.

Species	Wind Sector	$r2$	n	Ratio (units)	Ratio confidence limits (2σ)		Bottom-Up Emissions	Source	Base Year	α	αmin/max		Scaled Emissions	Scaled Emissions Min/Max		Top-Down Emissions (E_x)	E_x Min/Max	
					min	max					min	max		min	max		min	max
CO	N/E	0.75	44	9.3 (ppb ppm^{-1})	8.1	10.6	116.0 Gg	NEI08	2008	3.6	−10.5	11	120.1 Gg	103.8	128.4	65.8 Gg	50.1	81.7
	S	0.85	25	10.0 (ppb ppm^{-1})	6.7	13.3	362.1 Gg	NEI08	2008	1.7	−10.5	5	368.2 Gg	324.1	380.5	175.1 Gg	106.8	241.2
	Combined	0.81	68	9.4 (ppb ppm^{-1})	8.3	10.8	478.1 Gg	NEI08	2008	–	–	–	488.3 Gg	427.9	508.9	229.1 Gg	176.8	286.9
CH4	N/E	0.87	44	30.0 (ppb ppm^{-1})	24.1	33.3	64.3 Gg	CFRPS	2009	10	0	30	70.7 Gg	46.0	99.8	120.7 Gg	40.4	272.2
	S	0.69	26	9.8 (ppb ppm^{-1})	6.0	13.3	97.7 Gg	Edgar4.2	2008	1.7	0	5	99.3 Gg	97.7	102.6	98.1 Gg	55.2	137.6
C_2H_2	N/E	0.80	39	43.3 (ppt ppm^{-1})	36.2	59.3	0.172 Gg	NEI05	2005	11.6	0	35	0.192 Gg	0.172	0.232	0.284 Gg	0.210	0.403
	S	0.83	24	47.9 (ppt ppm^{-1})	37.0	58.0	0.544 Gg	NEI05	2005	5.2	0	16	0.572 Gg	0.544	0.629	0.776 Gg	0.541	1.001
	Combined	0.81	63	43.7 (ppt ppm^{-1})	38.3	55.4	0.687 Gg	NEI05	2005	–	–	–	0.764 Gg	0.716	0.861	0.995 Gg	0.760	1.326
BENZ	N/E	0.85	39	32.3 (ppt ppm^{-1})	27.1	38.9	0.468 Gg	NEI08	2008	3.6	0	11	0.485 Gg	0.468	0.518	0.64 Gg	0.22	1.44
	S	0.78	24	19.5 (ppt ppm^{-1})	16.6	25.0	1.28 Gg	NEI08	2008	1.7	0	5	1.30 Gg	1.28	1.34	0.95 Gg	0.71	1.28
i-C_5H_{12}	N/E	0.78	39	317.2 (ppt ppm^{-1})	243.3	456.0	4.4 Gg	CFRPS	2009	10	0	30	4.8 Gg	1.0	9.6	5.8 Gg	1.9	13.4
	S	0.83	23	92.7 (ppt ppm^{-1})	63.1	116.1	5.96 Gg	NEI05	2005	5.2	0	15.6	6.3 Gg	6.0	6.9	4.2 Gg	2.6	5.5
n-C_5H_{12}	N/E	0.78	39	332.5 (ppt ppm^{-1})	238.2	487.0	3.4 Gg	CFRPS	2009	10	0	30	3.7 Gg	1.0	8.5	6.0 Gg	1.8	14.1
	S	0.76	23	70.2 (ppt ppm^{-1})	47.7	98.8	4.52 Gg	NEI05	2005	5.2	0	15.6	4.8 Gg	4.5	5.2	3.1 Gg	2.0	4.6
n-C_4H_{10}	N/E	0.75	39	1126.4 (ppt ppm^{-1})	764.4	1497.7	11.4 Gg	CFRPS	2009	10	0	30	12.5 Gg	5.0	23.7	16.5 Gg	4.7	37.7
	S	0.70	23	191.6 (ppt ppm^{-1})	104.3	237.9	9.7 Gg	NEI05	2005	5.2	0	15.6	10.2 Gg	9.7	11.2	6.9 Gg	3.5	9.1
C_3H_8	N/E	0.76	39	2529.7 (ppt ppm^{-1})	1758.6	3462.3	26.1 Gg	CFRPS	2009	10	0	30	28.7 Gg	15.0	55.8	28.0 Gg	8.3	64.6
	S	0.55	23	412.7 (ppt ppm^{-1})	220.9	496.8	1.2 Gg	NEI05	2005	5.2	0	15.6	1.3 Gg	1.2	1.4	11.3 Gg	5.6	14.5
CO_2	N/E	–	–	– –	–	–	2.94 Tg C	Vulcan2.0	2002	2.8	–	–	3.02 Tg C	2.42	3.63	3.60 Tg C	1.10	6.80
	S	–	–	– –	–	–	7.27 Tg C	Vulcan2.0	2002	2.8	–	–	7.47 Tg C	5.98	8.97	– –	–	–

ACPD
13, 1609–1672, 2013

ACPD
13, 1609–1672, 2013

Constraints on emissions in the Colorado Front Range
B. W. LaFranchi

Table 2. Summary of trace gas lifetimes and major emission sources influencing observations at BAO (Watson et al., 2001; Pétron et al., 2012).

Species	Atmospheric Lifetime[a]	Major sources near BAO
carbon monoxide (CO)	49 days	on-road and non-road gasoline combustion
methane (CH_4)	6.9 yr	oil and gas systems[b], waste water treatment, landfills, cattle feed lots
acetylene (C_2H_2)	17 days	mobile sources (combustion)
benzene (C_6H_6)	10 days	mobile sources (combustion and evaporative), oil and gas systems
iso-pentane (i-C_5H_{12})	3.0 days	mobile sources (combustion and evaporative), oil and gas systems
n-pentane (n-C_5H_{12})	3.1 days	oil and gas systems
n-butane (n-C_4H_{10})	4.9 days	oil and gas systems
propane (C_3H_8)	12 days	oil and gas systems

[a] Atmospheric lifetimes estimated for [OH] = 1 × 10^6 cm^{-3} using published rate constant data (Atkinson et al., 2006; NASA, 2006).

[b] Sources include condensate tanks, well drilling and completion, distribution systems, refineries.

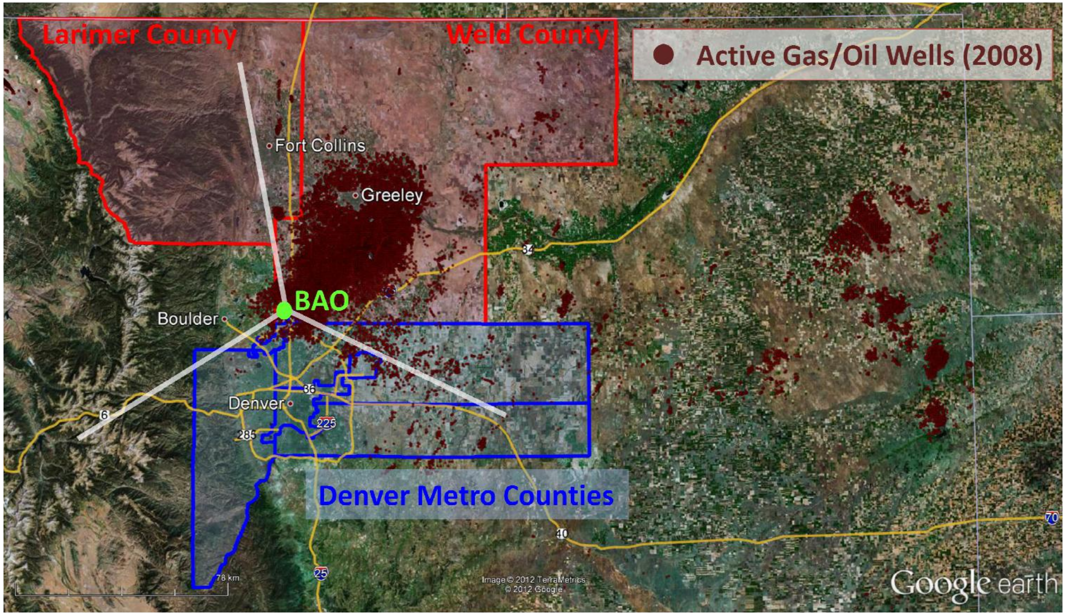

Fig. 1. Map of northwest Colorado showing the BAO tower and the distribution of active oil and gas wells (SkyTruth, 2008). Also shown are the three wind sectors used to filter the data set for emission estimates in Weld/Larimer counties (North and East) and in the Denver metro counties (South). The Denver metro counties include Denver, Broomfield, Adams, Arapahoe, and Jefferson.

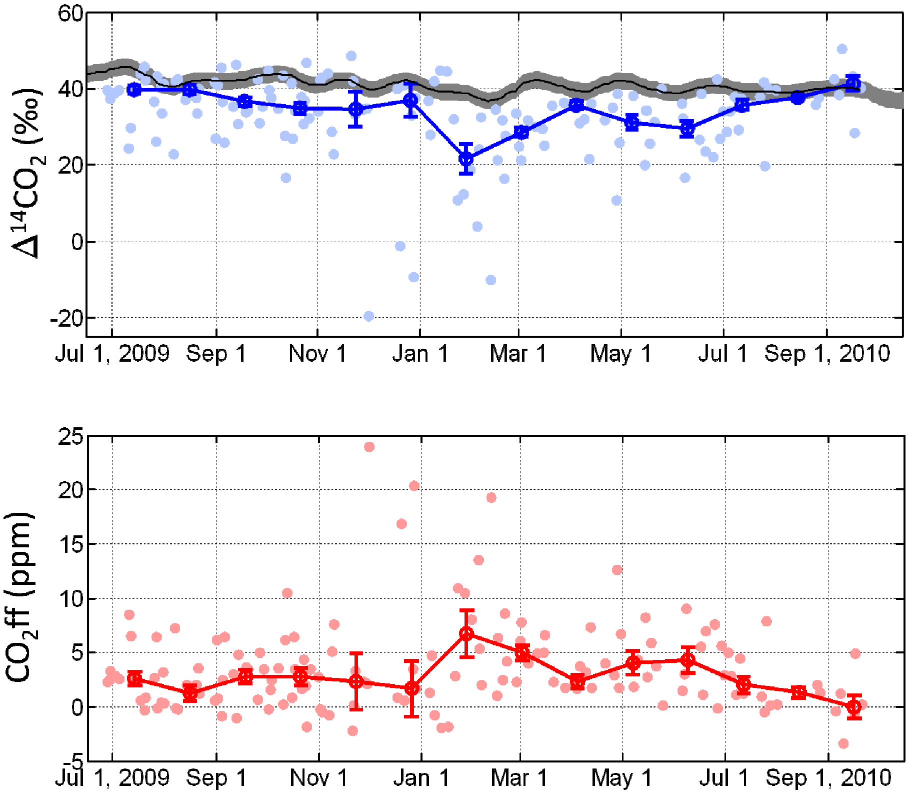

Fig. 2. Time series of $^{14}CO_2$ (above panel) and CO_2ff (below panel) from 145 discrete whole air samples (filled circles) collected at the BAO tower. Uncertainty in each $^{14}CO_2$ measurement is ±2.2‰, which translates to an uncertainty in each CO_2ff observation of 1.2 ppm (see Sect. 3.1). Thirty day binned medians are shown as open circles in both panels, with error bars representing the standard error of the mean (1σ) for each 30 day bin. Also shown in the above panel is the $^{14}CO_2$ background as observed at NWR (black line) (Turnbull et al., 2007; Lehman et al., 2012), with the uncertainty envelope represented by the grey shaded region.

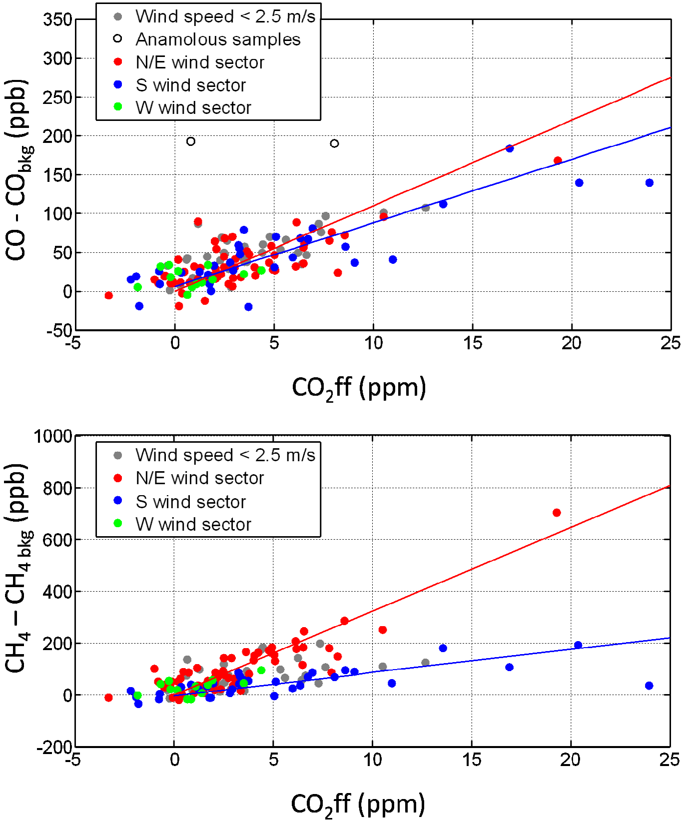

Fig. 3. Correlation plots of CO (above panel) and CH_4 (below panel) enhancements (with respect to background observations) with CO_2ff. Data are separated into one of three wind sectors (north and east: red; south: blue; and west green), except in cases where average wind speeds were below 2.5 m s^{-1} over the 30 min prior to sampling. Best-fit lines are shown for the N/E and S wind sectors (correlation coefficients are given in Table 1). In the above panel, two points are shown as open circles which are omitted from our analysis (see Sect. 2.5).

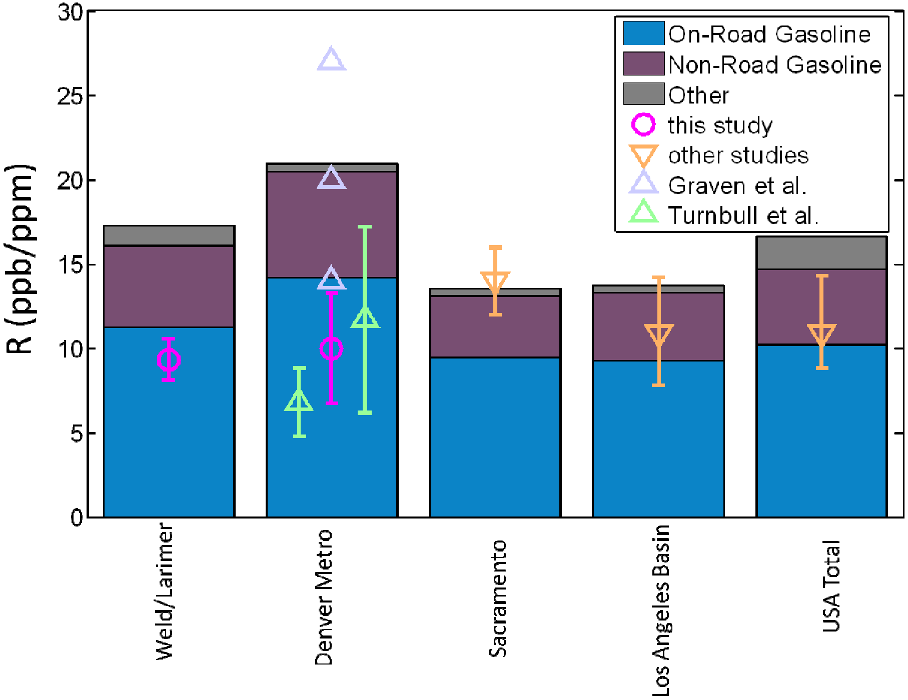

Fig. 4. A comparison of CO/CO_2ff ratios observed or estimated in various US locations. The bars are calculated from bottom-up emissions estimates (NEI08 CO and Vulcan2.2 CO_2) and color-coded by the contribution of different sectors to the total CO emissions: on-road gasoline, non-road gasoline, and other. Observations from each location are shown, including those from our observations at BAO (split into Weld/Larimer and Denver metro influence based on wind sector) and observations from other studies: Denver, Turnbull et al., 2006; Graven et al., 2009), Sacramento (Turnbull et al., 2011), LA Basin (which includes Los Angeles, Riverside, Orange, and San Bernardino counties) (Djuricin et al., 2010), and for the continental US (Miller et al., 2012).

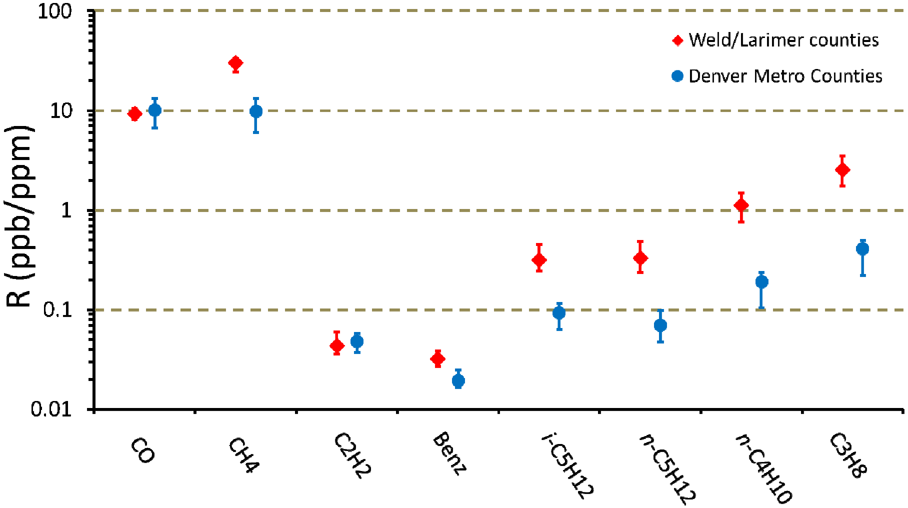

Fig. 5. Observed tracer/CO_2ff ratios from Weld County (N/E wind sector, red diamonds) and the Denver metro counties (S wind sector, blue circles). Ratios are calculated as the median of the point-by-point ratios for all data where CO_2ff was detected above 1.2 ppm, as described in Sect. 3.3. Uncertainties in the median ratios are the 95 % confidence intervals, defined as the 2.5–97.5 percentile range ($\sim 2\sigma$ confidence) from a distribution of 500 median estimates from a randomized re-sampling of the data (boot-strapping with replacement). Note that the figure is presented using a logarithmic scale.

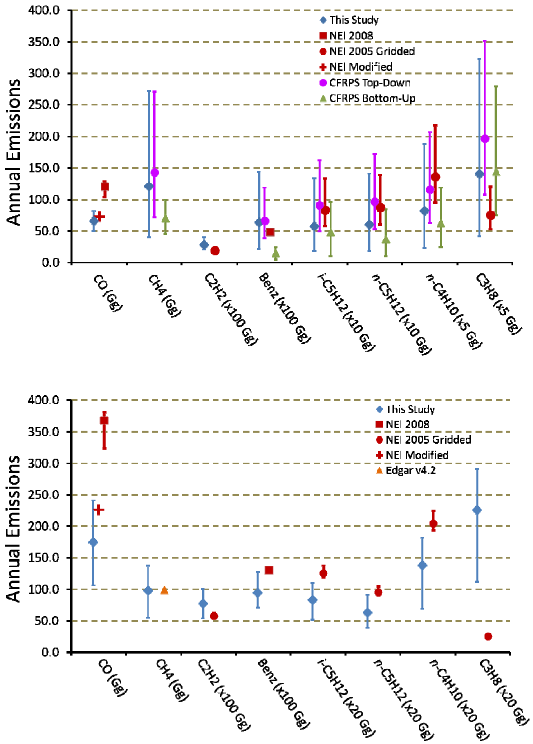

Fig. 6. Emissions estimates from Weld County (above panel) and the Denver metro counties (below panel). Top-down emissions, calculated using Eq. (4), are shown as blue diamonds, with uncertainties given as described in Sect. 3.3. Bottom-up emissions estimates are included for comparison for each species, making use of NEI, EDGAR, and CFRPS (Pétron et al., 2012) inventories. Also shown are the top-down estimates from the CFRPS for CH_4, Benzene, and the alkanes in Weld County. The CFRPS error bars (both bottom-up and top-down) are related to uncertainties in the VOC profiles for specific emission sources related to the oil and gas industry in Weld County. Note the differences in units for the different trace gases.

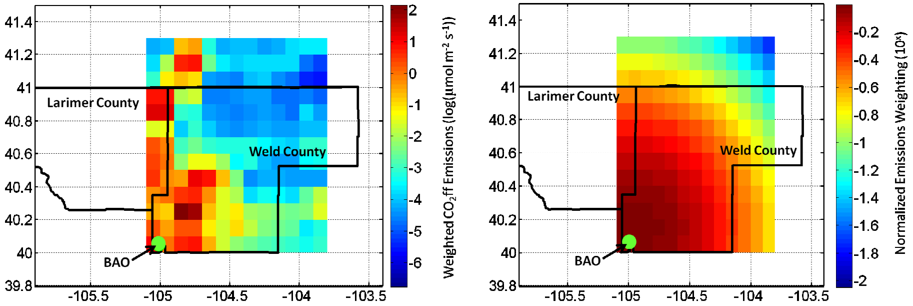

Fig. 7. Weighted Vulcan CO$_2$ff emissions (scaled to 2009–2010) (left panel) and weighting function (right panel) for a theoretical observation footprint for N/E wind sector observations.

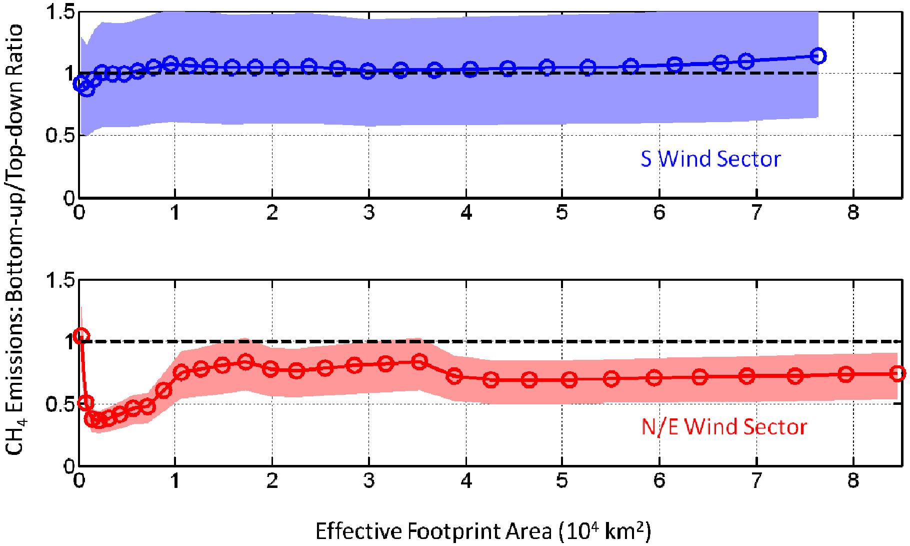

Fig. 8. Ratio of bottom-up (EDGARv4.2) to top-down emissions estimates across an expanding hypothetical footprint for the South wind sector (top) and the North/East wind sector (bottom). A value of one means perfect agreement between bottom-up and top-down estimates. Shaded areas reflect the uncertainties in top-down emissions estimates only.

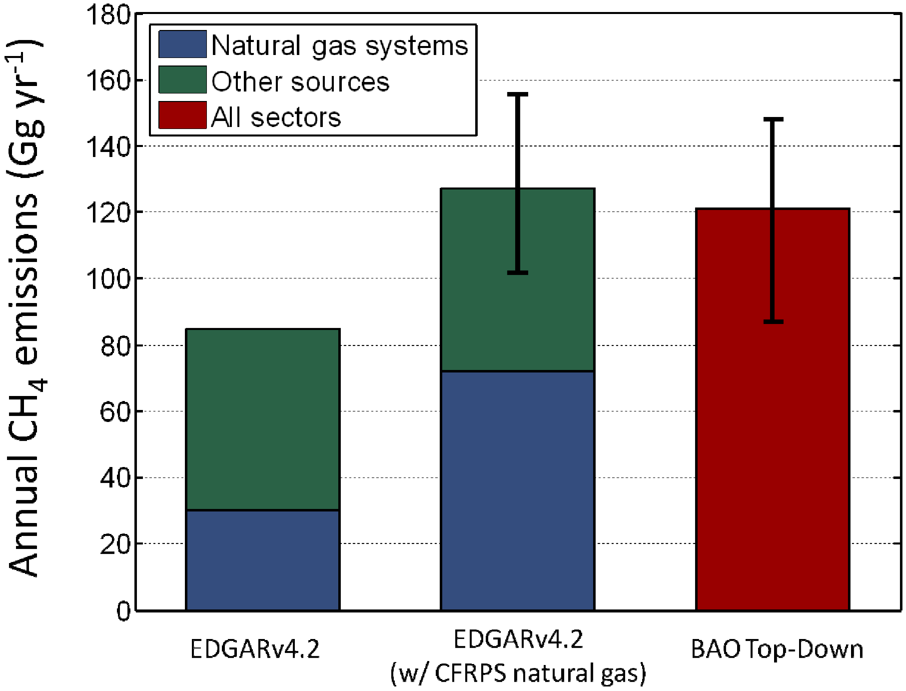

Fig. 9. Annual CH_4 emissions for N/E wind sector for 2010. Figure shows a comparison of the EDGARv4.2 inventory, the EDGARv4.2 inventory using the CFRPS bottom-up estimate for the oil and gas sector, and the top-down estimate using observations at BAO. Error bar for the EDGARv4.2/CFRPS combined estimate reflects uncertainty in the CFRPS estimate. Error bar on the top-down estimate reflects the observed uncertainty, as propagated through Eq. (4), but does not include the uncertainty in the geographic area influencing observations at BAO. See Sects. 3.3.4 and 4.2 for a detailed discussion.